

University of West Bohemia
Faculty of Electrical Engineering
Department of Applied Electronics and Telecommunications

MASTER THESIS

Simulation of a double ridge horn and a log-periodic dipole antenna
for EMC measurement

Author: Eugen Born, B. Eng.

Supervisor: Ing. Zdeněk Kubík, Ph.D.

Pocking, 08.02.2018

Declaration

Name of the student: Born Eugen
First corrector at the university: Ing. Zdeněk Kubík, Ph.D.
Second corrector at the university: Prof. Dr. rer.nat. Peter Jüttner
Subject of the master thesis:
Simulation of a double ridged horn antenna and a log-per antenna for EMC measurement

I hereby declare that I wrote the master thesis on my own, not yet otherwise presented for examination purposes, none other than those indicated sources or aids used as well as verbatim and analogous quotes as have characterized such.

Pocking, 08.02.2018

Born Eugen

Prologue / Acknowledgments

This final master thesis has been created as part of a double degree at TH-Deggendorf and at the University of West Bohemia, Czech Republic. In the period between August 2017 and January 2018 I got acquainted with the bought simulation software CST MWS, calculated, constructed two antennas and simulated their functionality. This research has been supported by the Ministry of Education, Youth and Sports of the Czech Republic under the RICE New Technologies and Concepts for Smart Industrial Systems, project No. LO1607. I would like to thank all those who supported and motivated me.

I would like to sincerely thank Prof. Dr. rer. nat. Peter Jüttner for his support in applying for the master's thesis at the University of West Bohemia.

Thanks to the University of West Bohemia and Doc. Dr. Ing. Vjačeslav Georgiev. Very big thanks also to Ing. Zdeněk Kubík, who patiently and extensively answered my questions and was always on hand with help and advice.

My thanks also go to my parents for their mental support and the support in all my decisions.

Lastly, I would like to thank all those who were there for me during the time of writing this thesis, especially my newfound Erasmus friends.

I. Contents

II. List of Figures	iii
III. List of Tables	iv
IV. Description of abbreviation	v
1. Introduction	1
1.1. Electromagnetic Compatibility.....	1
1.2. Description of the thesis	2
2. Basic information	3
2.1. Types of Antennas	3
2.2. Antenna parameters	4
2.2.1. Frequency	4
2.2.2. Wavelength.....	4
2.2.3. Input impedance	4
2.2.4. VSWR and Reflected Power	5
2.2.5. Bandwidth.....	5
2.2.6. Directivity and Gain	6
2.2.7. Radiation Pattern	7
2.2.8. Wave types and its modes	7
2.2.9 Scaling and spacing constant for LPDA.....	8
2.2.10. S-parameters	9
2.3. Horn antennas	11
3. Basic parameters.....	12
3.1. DRHA wave guide and horn calculation.....	12
3.2. Coax Connector	16
3.3. Log-periodic antennas	16
3.4. Log-periodic antenna calculation	16
4. Design of antennas.....	18

4.1. Double ridged horn antenna	19
4.1.1. Waveguide	19
4.1.2. Cavity back and connector	20
4.1.3. Horn	21
4.1.4. Ridges	25
4.2. Log-periodic antenna calculation	25
5. Simulation and optimization.....	27
5.1. CST MWS Time domain solver	27
5.2. Finite Integration Technique (FIT) – Maxwell equations	27
5.3. Signals in time domain simulation	28
5.4. CST MWS settings	29
5.5. Mesh	30
5.6. Double ridged horn antenna	31
5.6.1. Parameter overview and optimization	31
5.6.2. Simulation results of DRHA.....	32
5.7. Log-periodic dipole antenna.....	33
5.7.1. Parameter overview and optimization	33
5.7.2 Simulation results of LPDA	36
6. Conclusion and further work	37
7. References	39
V. List of Annexes.....	42
A1. Table for determination of PEL_H and PEL_E	43
A2. Optimization of DRHA.....	44
A3. Characteristic of DRHA	46
A4. Characteristic of LPDA	49
A5. Technical drawing DRHA	52
A6. Technical drawing LPDA	53

II. List of Figures

Figure 1: Double ridged horn antenna [3]	2
Figure 2: Log-per dipole antenna [4]	2
Figure 3: Lobe formation [10].....	7
Figure 4: Field distribution H_{10}	8
Figure 5: Field distribution H_{20}	8
Figure 6: Field distribution H_{30}	8
Figure 7: Four S-parameters of a quadrupole [21].....	10
Figure 8: Typical electromagnetic horn antenna configurations [14].....	11
Figure 9: Waveguide with ridges	12
Figure 10: Front view DRHA.....	13
Figure 11: Side view DRHA	14
Figure 12: Connection between coax and ridges [18].....	16
Figure 13: LPDA geometry [19]	17
Figure 14: TE_{10} with f_{cutoff} : 0.75GHz	19
Figure 15: TE_{20} with f_{cutoff} : 5.27GHz	20
Figure 16: TE_{30} with f_{cutoff} : 6.4GHz	20
Figure 17: Cavity back	21
Figure 18: Horizontal cut	21
Figure 19: Function of signals in time domain solver.....	29
Figure 20: Port distribution E-field (left) and H-field (right).....	29
Figure 21: Mesh cells of DRHA	30
Figure 22: DRHA 3D view	32
Figure 23: DRHA 3D vertical cut view	32
Figure 24: DRGA final S_{11} -parameter	32
Figure 25: DRHA final VSWR-parameter.....	33

Figure 26: S_{11} of calculated design.....	33
Figure 27: Different s-values.....	33
Figure 28: Different Lstub-values	34
Figure 29: Different d-values	34
Figure 30: S_{11} after 'simple' optimization	34
Figure 31: Different a_n - and d_n -values.....	35
Figure 32: LPDA 3D view	36
Figure 33: LPDA final S_{11} -parameter	36
Figure 34: LPDA final VSWR-parameter.....	36
Figure 35: Calculated result of DRHA.....	44
Figure 36: Different d for DRHA.....	44
Figure 37: Different b for DRHA.....	44
Figure 38: Different b_r for DRHA	44
Figure 39: Different c_w for DRHA	45
Figure 40: Different l_{con} for DRHA.....	45
Figure 41: Final result for DRHA	45

III. List of Tables

Table 1: Types of antenna [6]	3
Table 2: The $z(y)$ function values describe the shape of the ridge.....	25
Table 3: DRHA parameter overview	31
Table 4: LPDA parameter overview	35
Table 5: DRHA, LPDA advantages and disadvantages.....	37

IV. Description of abbreviation

Abbreviation	Unit	Description	Used
ATL	dB	Attenuation	p. 21
AC	-	Alternate currency	p. 3
CST MWS	-	CST Microwave Studio	p. 2, 18, 24, 26, 29, 30, 34, 36
DRHA	-	Double ridged horn antenna	p. 2, 11, 13, 29, 30, 31, 32, 41, 42, 43
EMC	-	Electromagnetic compatibility	p. 1, 2
ETL	-	Electrotechnical laboratory	p. 1
FIT	-	Finite Integration Technique	p. 26, 27
LPDA	-	Log-periodic dipole antenna	p. 2, 8, 9, 16, 29, 34, 35, 36, 46
PEL	dB	Phase error lost	p. 14, 21, 22, 23, 40
RF	Hz	Radio frequency	p. 3
S_{11}	dB	Return loss	p. 9, 10, 18, 30, 31 - 36
S-Parameter	dB	Scattering Parameter	p. 9, 10, 29
TE	-	Transverse electric	p. 7, 8, 11, 19
TEM	-	Transverse electromagnetic	p. 7
TM	-	Transverse magnetic	p. 7
VSWR	-	Voltage standing wave ratio	p. 5, 19, 31, 32, 33, 35

1. Introduction

Since the first demonstration of wireless technology in 1886 by Heinrich Hertz and its first practical radio application by Guglielmo Marconi in 1901, the antenna has been a key building block in the construction of wireless communications systems. Antennas are used by humans daily, for example for communication, orientation, warfare and research. Since the days of Hertz, antennas have advanced from a simple wire dipole to more complex structures such as helical antennas, parabolic reflectors, Yagis, microstrip patch arrays, Double-ridged waveguide horns, and other.

1.1. Electromagnetic Compatibility

EMC or Electromagnetic Compatibility, is the interaction of electrical and electronic equipment with its electromagnetic environment, and with other equipment. All electronic devices have the potential to emit electromagnetic fields, and with the proliferation of electronic devices into everyday life, from the more obvious devices such as mobile phones and computers, to more mundane household appliances such as TVs and washing machines. A huge potential for devices to interfere with each other. Although not as prevalent in the media as food or child toy safety, there have been several well publicized cases where, because electromagnetic compatibility was not fully considered, products have had to be recalled or withdrawn from the market at great expense and damage to the reputation of the manufacturer. To prevent the occurrence of EMC problems, the UK government adopted stringent laws, first back in 1992, forcing all manufacturers and importers of electronic goods to ensure that their products are electromagnetically compatible [1].

The University of West Bohemia has a Electrotechnical laboratory — ETL that offers a variety of compliance and pre-compliance tests of electronic devices. Almost every device requires a different test-frequency. So they are antennas with a huge bandwidth required to save time and accelerate the tests.

1.2. Description of the thesis

The goal of this thesis is designed and modeled two antennas, a double ridged horn antenna (DRHA) and a log-periodic dipole antenna (LPDA), with a bandwidth from 1 GHz to 6 GHz with CST Microwave Studio (CST MWS) to be built in the near future and used for EMC tests. Both antennas are shown below in figure 1 and 2. The thesis beginning with basics of antenna theory and the antenna design, following with the design of a double ridged horn and a log-periodic antenna. The basic parameters will be simulated with the program CST MWS.

CST MWS is a specialist tool for the 3D electromagnetic simulation of high frequency components and enables the fast and accurate analysis of high frequency devices such as antennas, filters, couplers, planar and multi-layer structures and SI and EMC effects [2]. Finally, there is a short conclusion of the designed antennas.



Figure 1: Double ridged horn antenna [3]

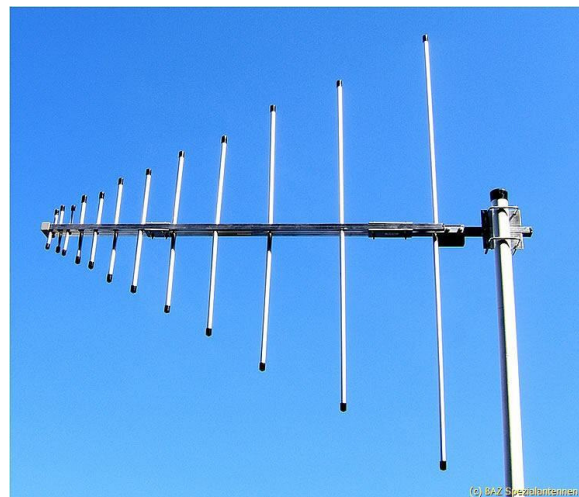


Figure 2: Log-per dipole antenna [4]

2. Basic information

An antenna is a specialized transducer that converts radio-frequency (RF) fields into alternating current (AC). There are two basic types: the receiving antenna, which intercepts RF energy and delivers AC to electronic equipment, and the transmitting antenna, which is fed with AC from electronic equipment and generates an RF field [5]. Usually one antenna is used for both applications.

2.1. Types of Antennas

In the following table are different types of antennas and their usage shown.

Type of antenna	Examples	Applications
Wire Antennas	Dipole antenna, Monopole antenna, Helix antenna, Loop antenna	Personal applications, buildings, ships, automobiles, space crafts
Aperture Antennas	Waveguide (opening), Horn antenna	Flush-mounted applications, air-craft, space craft
Reflector Antennas	Parabolic reflectors, Corner reflectors	Microwave communication, satellite tracking, radio astronomy
Lens Antennas	Convex-plane, Concave-plane, Convex-convex, Concave-concave lenses	Used for very high frequency applications
Micro strip Antennas	Circular-shaped, Rectangular shaped metallic patch above the ground plane	Air-craft, space-craft, satellites, missiles, cars, mobile phones etc.
Array Antennas	Yagi-Uda antenna, Micro strip patch array, Aperture array, Slotted wave guide array	Used for very high gain applications, mostly when needs to control the radiation pattern

Table 1: Types of antenna [6]

In general, to select the best antenna, designers should address the following specifications as a starting point: frequency, bandwidth, radiation pattern (peak gain and average gain), and size. The dimensions of a broadband antenna depend on its cut-off frequency. The operating medium (i.e. outdoors, indoors) of the antenna is also crucial.

2.2. Antenna parameters

The basic communication parameters are discussed in this chapter to have a better idea about the wireless communication using antennas. The wireless communication is done in the form of waves.

2.2.1. Frequency

According to the standard definition, “The rate of repetition of a wave over a particular period of time, is called as frequency.” Simply, frequency refers to the process of how often an event occurs.

$$f = \frac{1}{T} \text{ [Hz]}, \quad (1)$$

where T is time period in seconds. A periodic wave repeats itself after every time period. Frequency of periodic wave is nothing but the reciprocal of time period [7].

2.2.2. Wavelength

According to the standard definition, “The distance between two consecutive maximum points (crests) or between two consecutive minimum points (troughs) is known as the wavelength.”

$$\lambda = \frac{c}{f} \text{ [m]}, \quad (2)$$

Where c represents speed of light in vacuum ($c = 299\,792\,458$ m/s). The wavelength λ could be expressed in the units of length such as meters, feet or inches [7].

2.2.3. Input impedance

Input impedance Z_0 is defined as the impedance presented by an antenna at its terminals or the ratio of the voltage to current at a pair of terminals or the ratio of the appropriate components of the electric to magnetic fields at a point [8].

To reduce signal reflections, it is important to have a matched connection. This means that the input impedance of the inputs, the characteristic impedance of the transmission line, and the load impedance all have to be equal in order to achieve maximum energy transfer between a wire or coaxial transmission line and an antenna. If the two impedance do not match, a reflected wave will be generated at the antenna terminal and travel back towards the energy source. This reflection of energy results in a reduction in the overall system efficiency [7].

2.2.4. VSWR and Reflected Power

If the impedance of the antenna, the transmission line and the circuitry do not match with each other, then the power will not be radiated effectively. Instead, some of the power is reflected back. The key features are: The term, which indicates the impedance mismatch is VSWR. VSWR stands for Voltage Standing Wave Ratio.

$$VSWR = \frac{V_{max}}{V_{min}} = \frac{1 + |\Gamma|}{1 - |\Gamma|} [-]. \quad (3)$$

The higher the impedance mismatch, the higher will be the value of VSWR. The ideal value of VSWR should be 1:1 for effective radiation. Reflected power is the power wasted out of the forward power. The reflection coefficient is typically represented with a Γ (capital gamma) Both reflected power and VSWR indicate the same thing [7].

2.2.5. Bandwidth

The signal when transmitted or received, is done over a range of frequencies. This particular range of frequencies is allotted to a particular signal, so that other signals may not interfere in its transmission. Bandwidth is the band of frequencies between the higher and lower frequencies over which a signal is transmitted. The bandwidth once allotted, cannot be used by others. The whole spectrum is divided into bandwidths to allot to different transmitters [7].

$$B = f_{high} - f_{low} [Hz]. \quad (4)$$

2.2.6. Directivity and Gain

According to the standard definition, “The ratio of maximum radiation intensity of the subject antenna to the radiation intensity of an isotropic or reference antenna, radiating the same total power is called the directivity.”

An Antenna radiates power, but the direction in which it radiates matters much. The antenna, whose performance is being observed, is termed as subject antenna. Its radiation intensity is focused in a particular direction, while it is transmitting or receiving. Hence, the antenna is said to have its directivity in that particular direction. The ratio of radiation intensity in a given direction from an antenna to the radiation intensity averaged over all directions, is termed as directivity.

$$\text{Directivity } D = \frac{\text{Maximum radiation intensity of subject antenna}}{\text{Radiation intensity of an isotropic antenna}} \text{ [dBi]}. \quad (5)$$

According to the standard definition, “Gain of an antenna is the ratio of the radiation intensity in a given direction to the radiation intensity that would be obtained if the power accepted by the antenna were radiated isotropically.”

$$G = \eta \cdot D \text{ [dB]}, \quad (6)$$

simply, gain of an antenna takes the directivity of antenna into account along with its effective performance. If the power accepted by the antenna was radiated isotropically (that means in all directions), then the radiation intensity we get can be taken as a referential. The term antenna gain describes how much power is transmitted in the direction of peak radiation to that of an isotropic source. Gain is usually measured in decibel, a logarithmic unit used to express the ratio of a value to a reference value, here signal from input to the output. Unlike directivity, antenna gain takes the losses that occur also into account and hence focuses on the efficiency η [7].

2.2.7. Radiation Pattern

When the power radiation intensity Φ and the power density P are presented on relative scales, they are identical and often are referred to as the antenna radiation pattern. The main or major lobe of the radiation pattern is in the direction of maximum gain. All other lobes are called side lobes or minor lobes. The lobe formation is shown in figure 3. There is another lobe, which is exactly opposite to the direction of main lobe. It is known as back lobe, which is also a minor lobe. A considerable amount of energy is wasted even here [11].

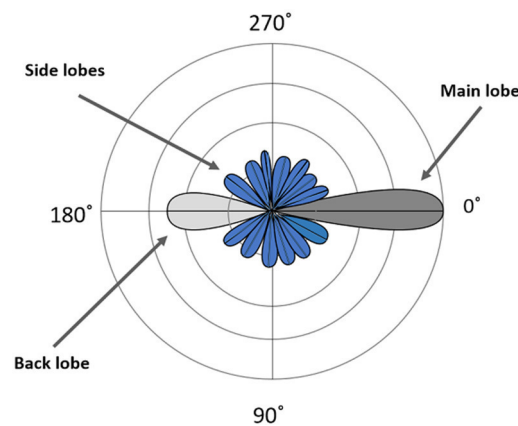


Figure 3: Lobe formation [10]

2.2.8. Wave types and its modes

There are different types of wave propagation and modes that can exist on general transmission lines and waveguides. Transmission lines that consist of two or more conductors may support transverse electromagnetic (TEM) waves, characterized by the lack of longitudinal field components. Such lines have a uniquely defined voltage, current, and characteristic impedance. Waveguides, often consisting of a single conductor, support transverse electric (TE) and/or transverse magnetic (TM) waves, characterized by the presence of longitudinal magnetic or electric field components [12]. In the type of waveguide handled in this thesis, it is possible to see the TE and the TM waves. The hollow rectangular waveguide can propagate TE and TM modes, but not TEM waves, since only one conductor is present. Transverse magnetic waves, also referred to as E-waves, are characterized by $E_z \neq 0$ (electric field) and $H_z = 0$ (magnetic field). Transverse electric waves, also referred to as H-waves are characterized by $E_z = 0$ and $H_z \neq 0$. The ground mode wave is the wave mode with the lowest cut-off frequency and most

common transmitted wave in rectangular waveguide. In rectangular waveguides, the ground mode is TE₁₀ or H₁₀.

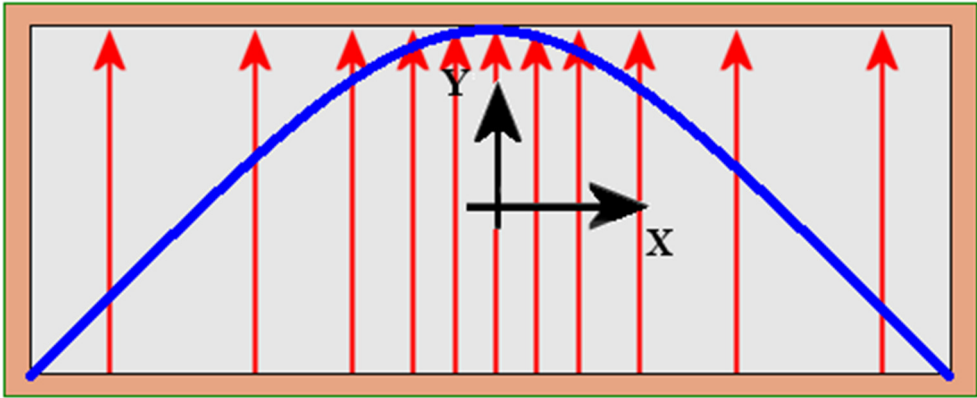


Figure 4: Field distribution H₁₀

It has this name because all electric fields are transverse to the direction of the propagation and has no longitudinal electric field. In general, they are referred to as TE_{m_n} [11]. The field distribution T₁₀ wave can be observed in the Figure 4. It is clear that the maximum energy from the fields are concentrated in the middle. Figure 5 and 6 shows the two modes T₂₀ and T₃₀.

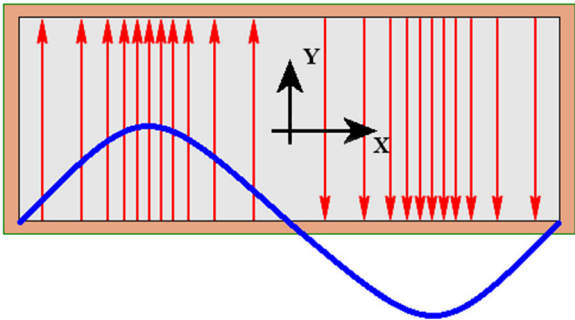


Figure 5: Field distribution H₂₀

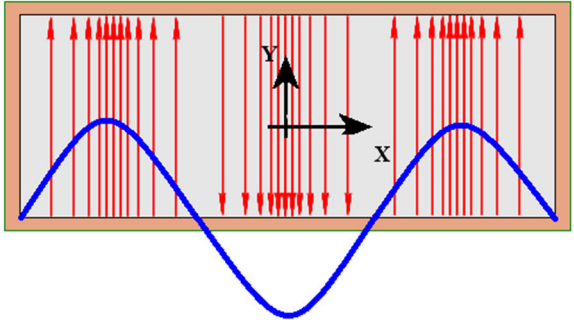


Figure 6: Field distribution H₃₀

2.2.9 Scaling and spacing constant for LPDA

Every log-periodic structure has a basic scaling cell where we scale every dimension throughout the antenna by a constant:

$$\frac{f_1}{f_2} = \frac{\lambda_2}{\lambda_1} = \tau [-]. \tag{7}$$

scaling constant $\tau < 1$

The antenna will scale exactly at the sequence of frequencies:

$$f_n = \frac{f_0}{\tau^n} \text{ [Hz]}. \quad (8)$$

We make the antenna periodic in the logarithm of frequency with every dimension scaled by τ from element to element. For any value of τ , we may determine the optimal value of the spacing constant σ :

$$\sigma_{opt} = 0.243 \cdot \tau - 0.051 \text{ [-]}. \quad (9)$$

The combination of a value for τ and its corresponding optimal value of σ yields the highest performance of which an LPDA is capable. For values of τ from 0.80 through 0.98, the value of optimal σ varies from 0.143 to 0.187, in increments of 0.00243 for each 0.01 change in τ . However, using the optimal value of σ usually yields a total array length that is beyond ham construction or tower/mast support capabilities. Consequently, amateur LPDAs usually employ compromise values of τ and σ that yield lesser but acceptable performance [13].

2.2.10. S-parameters

Scattering parameters, S-parameters, are frequency-dependent parameters of high-frequency circuits, components, devices and systems and represent the transmission and reflection values of the inputs and outputs. S-parameters are given as complex numbers in magnitude and phase, the amount in decibels (dB), the phase angle in degrees. They are dimensionless and belong to a given nomenclature. This nomenclature depends on order, resp. port number.

A one-port is a two connection device, a two pole, and is described by a single scatter parameter (S_{11}). A two-port corresponds to a quadrupole and is described by four S-parameters, S_{11} , S_{21} , S_{12} and S_{22} . This can be used to describe most circuits and RF modules. A three-port, three-port, is described by the nine S-parameters S_{11} , S_{12} , S_{13} , S_{21} , S_{22} , S_{23} , S_{31} , S_{32} and S_{33} and a four-port by sixteen S-parameters.

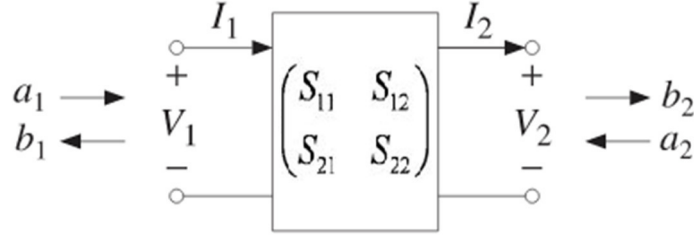


Figure 7: Four S-parameters of a quadrupole [21]

$$\begin{pmatrix} b_1 \\ b_2 \end{pmatrix} = \begin{pmatrix} S_{11} & S_{12} \\ S_{21} & S_{22} \end{pmatrix} \times \begin{pmatrix} a_1 \\ a_2 \end{pmatrix}. \quad (10)$$

The parameters S_{11} , S_{22} have the meaning of reflection coefficients, and S_{21} , S_{12} , the meaning of transmission coefficients. The S-parameter S_{11} represents the wave resistance-correct matching of the input to the impedance of the measuring line, which has 50 ohms or 75 ohms. A low S_{11} value indicates that the return loss is low. S_{21} is about the transmission and thus the insertion loss or gain that a multipole causes. For passive components with bidirectional properties, S_{12} corresponds to the S parameter S_{21} . And S_{22} is about adapting the output to the impedance of the measurement system [21].

The traveling wave variables a_1 , b_1 at port 1 and a_2 , b_2 at port 2 are defined in terms of V_1 , I_1 and V_2 , I_2 and a real-valued positive reference impedance Z_0 as follows:

$$a_1 = \frac{V_1 + Z_0 I_1}{2\sqrt{Z_0}}, \quad a_2 = \frac{V_2 - Z_0 I_2}{2\sqrt{Z_0}}, \quad (11)$$

$$b_1 = \frac{V_1 - Z_0 I_1}{2\sqrt{Z_0}}, \quad b_2 = \frac{V_2 + Z_0 I_2}{2\sqrt{Z_0}}. \quad (12)$$

Every single S-parameter can be obtained by the following equations:

$$S_{11} = \frac{b_1}{a_1}, \quad (13)$$

$$S_{12} = \frac{b_1}{a_2}, \quad (14)$$

$$S_{21} = \frac{b_2}{a_1}, \quad (15)$$

$$S_{22} = \frac{b_2}{a_2}. \quad (16)$$

The S-parameter S_{11} from two-port network theory is frequently also called return loss, but is actually equal to Γ .

2.3. Horn antennas

One of the simplest and probably the most widely used microwave antenna is the horn antenna. The horn antenna is widely used as a feed element for large radio astronomy, satellite tracking, and communication dishes found installed throughout the world.

In addition to its utility as a feed for reflectors and lenses, it is a common element of phased arrays and serves as a universal standard for calibration and gain measurements of other high gain antennas. Its widespread applicability stems from its simplicity in construction, ease of excitation, versatility, large gain, and preferred overall performance.

An electromagnetic horn can take many different forms (Figure 8). The horn antenna is nothing more than a hollow pipe of different cross sections, which has been tapered to a larger opening. The type, direction, and amount of taper can have a profound effect on the overall performance of the element as a radiator [14].

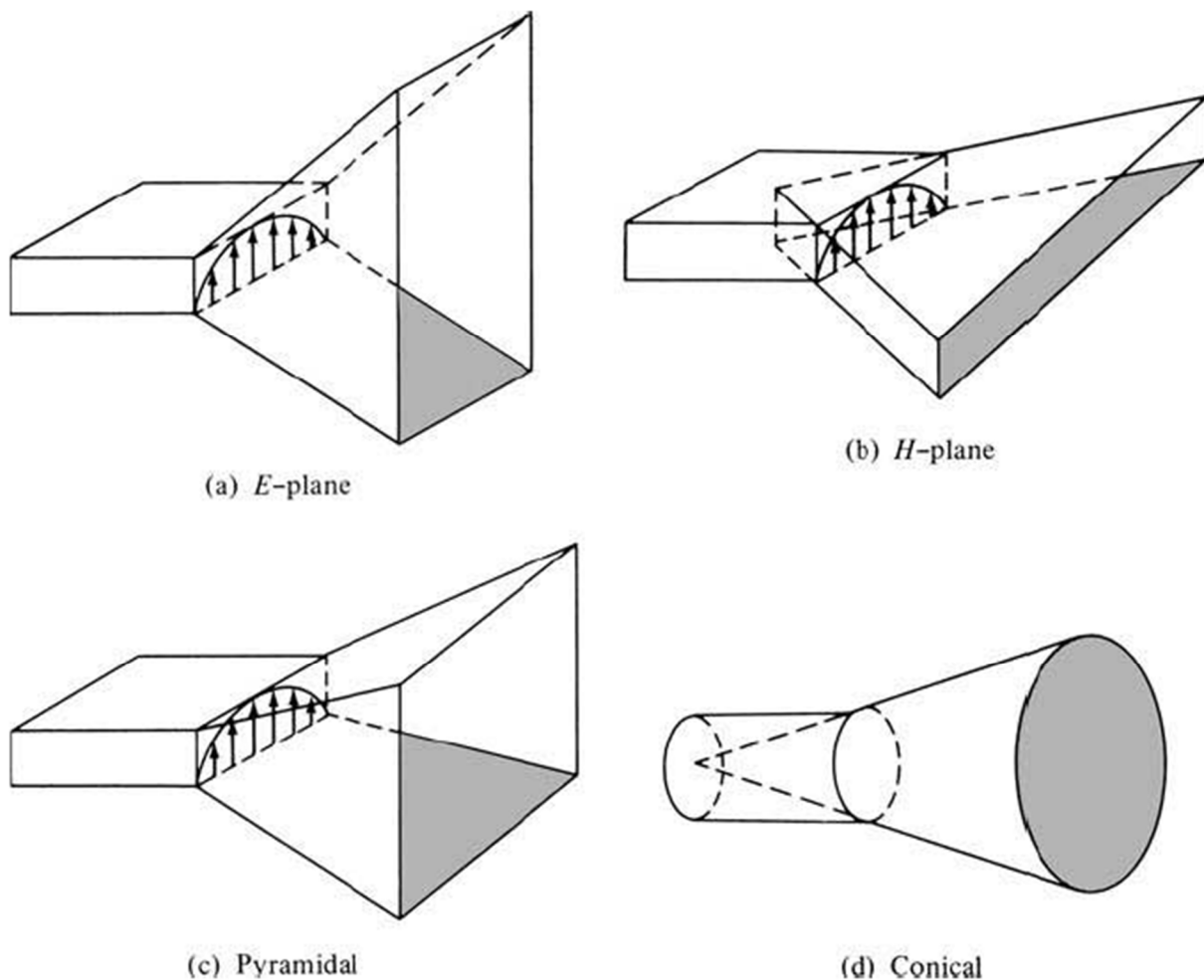


Figure 8: Typical electromagnetic horn antenna configurations [14]

3. Basic parameters

3.1. DRHA wave guide and horn calculation

A common way to increase the bandwidth of a waveguide is to introduce ridges in the middle of the waveguide that go along the propagation direction (Figure 9). Although the increase is significant, it happens at the expense of higher attenuation and lower power-handling capability. Introduction of the ridges mainly lowers the cut-off frequency of the TE_{10} mode from that of the unloaded guide, which is predicated on width alone. The reason for this can easily be explained when the field configuration in the guide at cut-off is investigated. At cut-off there is no longitudinal propagation down the guide. The waves simply travel back and forth between the side walls of the guide.

In fact, the guide can be viewed as a composite parallel plate waveguide of infinite width where the width corresponds to the direction of propagation of the normal guide. The TE mode cut-off occurs where this composite guide has its lowest-order resonant frequency. This occurs when there is only one E-field maximum across the guide which occurs at the center for a symmetrical ridge. Because of the reduced height of the guide under the ridge, the effective TE mode resonator is heavily loaded as though a shunt capacitor were placed across it. The cut-off frequency is thus lowered considerably [11].

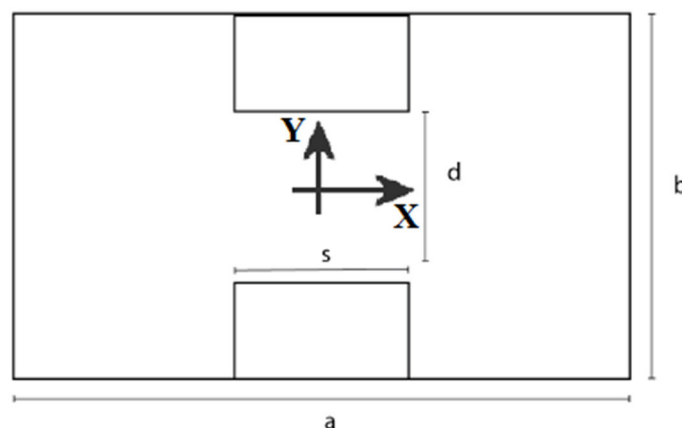


Figure 9: Waveguide with ridges

First of all, we are looking for the parameter a , the width of the waveguide. The third mode defines the upper cut-off frequency and thus the dimensions of the waveguide.

$$f_m = \frac{c}{2} \cdot \sqrt{\left(\frac{m}{a}\right)^2} \text{ [Hz]}. \quad (17)$$

The formula is changed to receive the parameter a .

$$a = \frac{m \cdot c}{2 \cdot f_m} \text{ [mm]}. \quad (18)$$

For the first approximation the following formula is used:

$$a \geq 2 \cdot b. \quad (19)$$

Going out of a we can find the other parameters. Its recommended to take following values.

$$0.01 \leq \frac{d}{b} \leq 1,$$

$$0 < \frac{b}{a} \leq 1,$$

$$0 \leq \frac{s}{a} \leq 0.45.$$

For $\frac{s}{a} > 0.45$, accuracy decreases rapidly because of the mounting influence of the side walls upon the field at the ridges [15]. There are no defined measurements for s and d . It is very helpful in this stage to use a simulation program to be able to find out the optimal proportion from height to width from the ridges.

The horn of the antenna is designed according to the procedure below. First it is designed the funnel of the antenna into which the ridge of the prescribed shape is then inserted.

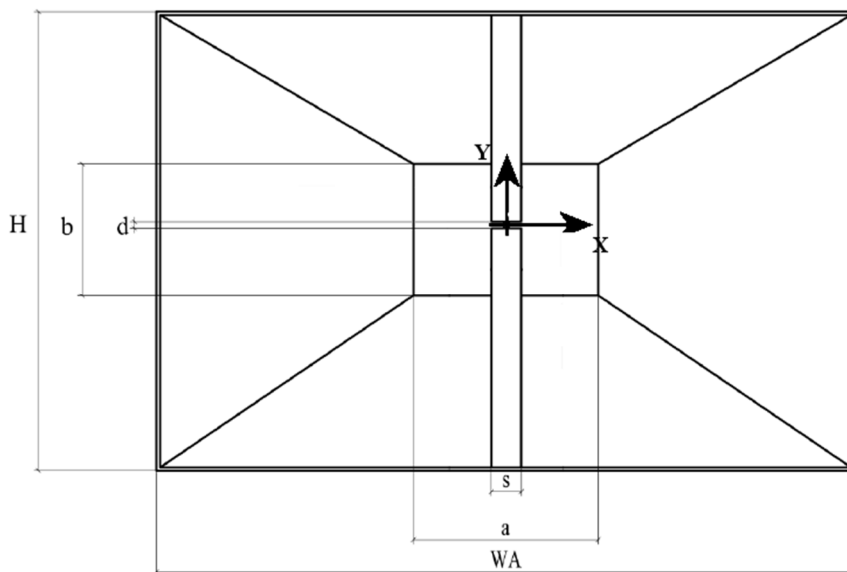


Figure 10: Front view DRHA

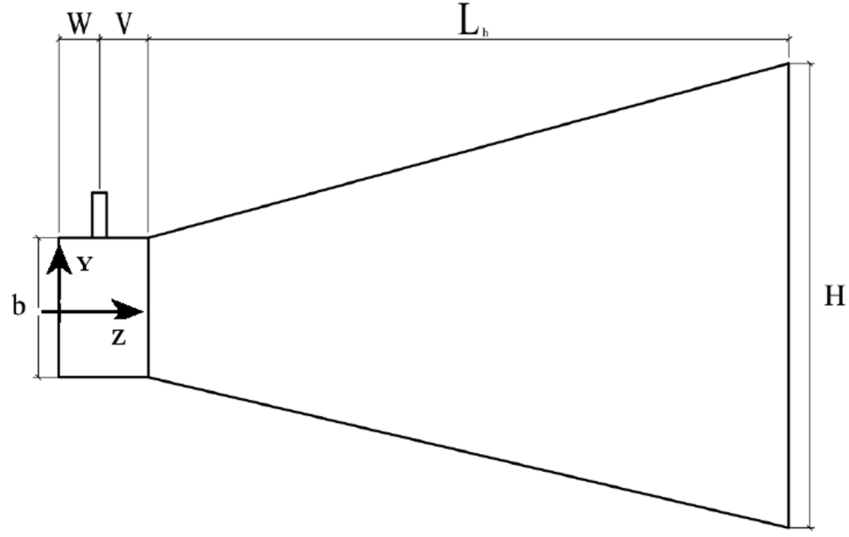


Figure 11: Side view DRHA

Knowing the required gain at a given frequency, you can calculate the dimension's apertures according to the following formulas. WA is the aperture width and H is the aperture height according to [16].

$$WA = 0.489 \cdot \sqrt{G} \cdot \lambda \text{ [mm]}, \quad (20)$$

$$H = 0.332 \cdot \sqrt{G} \cdot \lambda \text{ [mm]}. \quad (21)$$

Further, it is necessary to determine the horizontal radius R_h :

$$R_h = 0.0746 \cdot G \cdot \lambda \text{ [mm]}. \quad (22)$$

With knowledge of the horizontal radius R_h , it is possible to calculate the aperture length L .

$$L_h = \frac{WA - a}{WA} \cdot \sqrt{R_h^2 - \frac{WA^2}{4}} \text{ [mm]}. \quad (23)$$

It is also necessary to determine the vertical radius R_e .

$$R_e = \frac{H}{H - b} \cdot \sqrt{L_h^2 - \frac{(H - b)^2}{4}} \text{ [mm]}. \quad (24)$$

To determine the phase error losses, the distribution values must first be calculated quadratic phase constants S_E for E-plane and S_H for H-plane.

$$S_E = \frac{H^2}{8 \cdot \lambda \cdot R_e} [mm], \quad (25)$$

$$S_H = \frac{WA^2}{8 \cdot \lambda \cdot R_h} [mm]. \quad (26)$$

Using these values, we deduct PEL_E and PEL_H values from the attached table A1. From previous relationships, it is possible to determine the actual directivity of the calculated horn. Usually the directivity will be equated to gain, since the wall losses are very small. Although we can use the fixed-amplitude taper loss of 0.91 dB to determine the aperture efficiency of a rectangular horn.

$$G_{act[dB]} = 10 \log \left(\frac{4\pi \cdot H \cdot WA}{\lambda^2} \right) - ALT - PEL_H - PEL_E [dB]. \quad (27)$$

The latest calculation is then the calculation of the "new" gain.

$$G_{new} = \frac{G_{req} \cdot G_d}{G_{act}} [-]. \quad (28)$$

G_{req} is the required gain, G_d is the original gain of the apparatus used in relationships, G_{act} is the recalculated (actual) gain. It is an iterative process to calculate the correct measurements for the horn. The next step is to use G_{new} for calculating a new H and WA . The iterative process ends when G_{new} reached G_{req} .

The next step is to insert the ridge. The ridge profile is described by the equation of function $z(y)$, assumed that the ridge is located along the z axis.

$$z(y) = z(0) \cdot e^{k \cdot y} [mm]. \quad (29)$$

$z(0)$ is half of the gap between the ridges at the beginning of the horn. k is the constant obtained by the equation according to [17]:

$$k = \frac{1}{L} \cdot \ln \left(\frac{z(L)}{z(0)} \right) [mm^{-1}], \quad (30)$$

where L is the length of the horn.

3.2. Coax Connector

A very important part of an antenna is its feeding point. In high frequency range, the antenna is often connected to the source with a coaxial cable. The maximum and most efficient transfer of electrical energy occurs when the source impedance is matched to the load impedance. If both characteristic impedances are the same, the energy from the transmitter travels almost without power loss throughout the transmission line into the antenna. The transition between coaxial probe and the double-ridged waveguide is important for the return loss performance of the horn antenna [18].

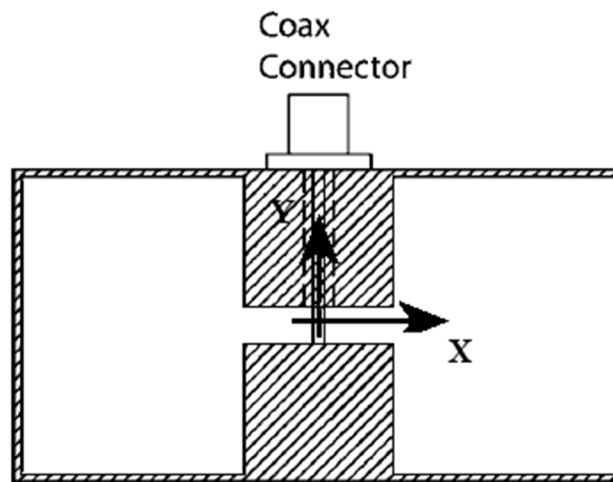


Figure 12: Connection between coax and ridges [18]

3.3. Log-periodic antennas

Log-periodic antennas were developed in the late 1950s out of modifications to the conical spiral concept of an antenna specified by angles. All continuously scaled antennas radiate circular polarization. The point of constant beamwidth rotates with frequency. We can build linearly polarized self-scaling antennas only with structures that scale at discrete frequency intervals. The pattern characteristics will ripple between exact scaling frequencies, but with closely spaced scaling the antenna is practically frequency independent [19].

3.4. Log-periodic antenna calculation

This LPDA calculation is mainly based on the design procedure as described by L. B. Cebik, W4RNL (SK) in the 21st edition of 'The ARRL Antenna Handbook' [13].

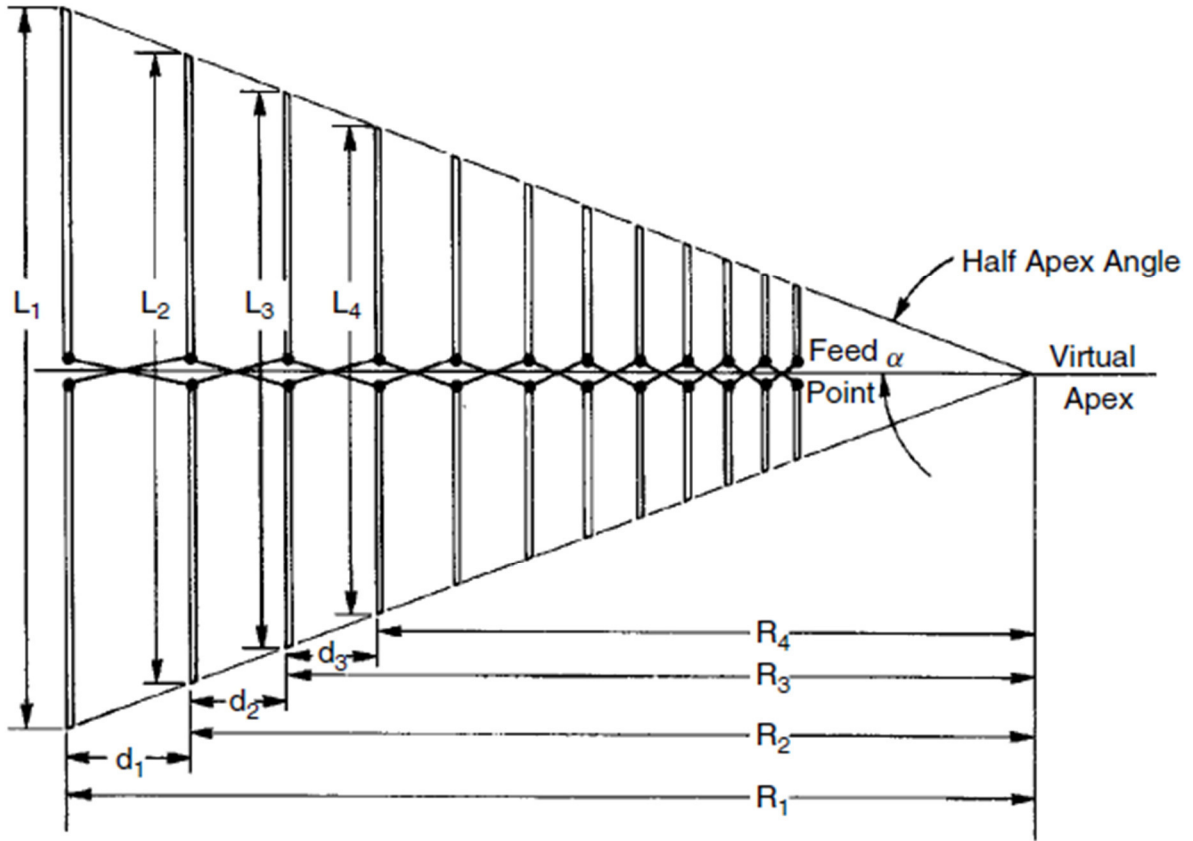


Figure 13: LPDA geometry [19]

For proper sizing, the LPDA parameters should be within the following limits:

$$0.81 \leq \tau \leq 0.95,$$

$$0.1 \leq \sigma \leq 0.2,$$

$$50 \Omega \leq R_0 \leq 300 \Omega,$$

$$4^\circ \leq \alpha \leq 20^\circ.$$

After choosing τ and σ the structure opening angle can be determined:

$$\alpha_{rad} = \arctan \frac{1 - \tau}{4 \cdot \sigma} [-], \quad (31)$$

$$\alpha = \alpha_{rad} \cdot \frac{180^\circ}{\pi} [^\circ]. \quad (32)$$

Further the relative operating bandwidth B , relative bandwidth of the active region B_{ar} and the relative bandwidth of the structure B_S will be calculated:

$$B = \frac{f_n}{f_1} [-], \quad (33)$$

$$B_{ar} = 1.1 + 30.8 \cdot (1 - \tau) \cdot \sigma [-], \quad (34)$$

$$B_S = B \cdot B_{ar} [-]. \quad (35)$$

Number of elements can be obtained with:

$$N = 1 + \frac{\log(B_S)}{\log\left(\frac{1}{\tau}\right)} [-]. \quad (36)$$

The width of the active zone depends on the extent of the longest dipole of the antenna.

$$L_1 \approx \frac{c}{2 \cdot f_1} = \frac{\lambda_{max}}{2} [\text{mm}]. \quad (37)$$

The length of each dipole and the total sum of all dipole lengths is calculated by

$$L_n = \tau^{n-1} \cdot L_1 [\text{mm}], \quad (38)$$

$$L_{total} = \sum_{i=1}^n L_i [\text{mm}]. \quad (39)$$

To calculate the element distances d and element diameter a following formula are needed:

$$d_n = \tau^{n-1} \cdot d_1 [\text{mm}], \quad (40)$$

$$d_1 = 2 \cdot \sigma \cdot L_1 [\text{mm}], \quad (41)$$

$$a_1 = \frac{L_1}{S} [\text{mm}]. \quad (42)$$

The boom length and the length of terminating stub can be obtained by

$$L = \sum_{i=1}^{n-1} d_i [\text{mm}], \quad (43)$$

$$l_{stub} = \frac{\lambda_{max}}{8} [\text{mm}]. \quad (44)$$

4. Design of antennas

This chapter deals with the design of antennas with a working band of 1.0 GHz to 6 GHz. After calculating the antenna dimensions according to the relationships mentioned in the previous chapters an antenna model in the CST MWS is created.

To reach an adjustment factor of $S_{11} < -10$ dB in a given work band its necessary to optimize the calculated dimensions.

4.1. Double ridged horn antenna

To get a smoother transition at the limits of S_{11} and VSWR the calculation will be done with increased limits of 0.7 GHz and 6.5 GHz.

4.1.1. Waveguide

To reach the upper limit frequency of 6 GHz we use the formula (18) and mode:3.

$$a = \frac{m \cdot c}{2 \cdot f_m} = \frac{3 \cdot 3 \cdot 10^8}{2 \cdot 6.5 \cdot 10^9} = 0.069m = 69 \text{ mm.}$$

For further calculation $a = 70 \text{ mm}$ will be used. The length of the waveguide has no big influence to the simulation and is chose randomly to 25 mm . To get parameter b the relation (19) will be applied and thus we get $b \leq 35 \text{ mm}$. By using the recommended value for $\frac{s}{a} = 0.3$ and $\frac{d}{b} = 0.1$, s is 21 mm and d is 3.5 mm . The layout of the different modes with their associated cut-off frequencies are displayed in Figure 14 to 16.

For further calculations, it is necessary to know the wavelength, which can be calculated by the relation (2):

$$\lambda = \frac{c}{f} = \frac{3 \cdot 10^8}{6.5 \cdot 10^9} = 0.046 \text{ m} = 46 \text{ mm.}$$

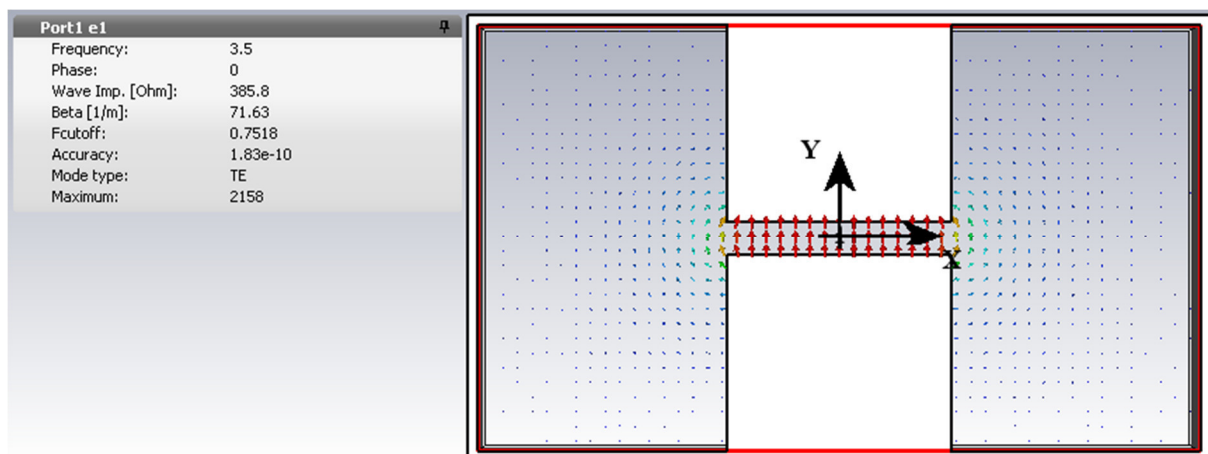


Figure 14: TE_{10} with $f_{\text{cutoff}}: 0.75\text{GHz}$

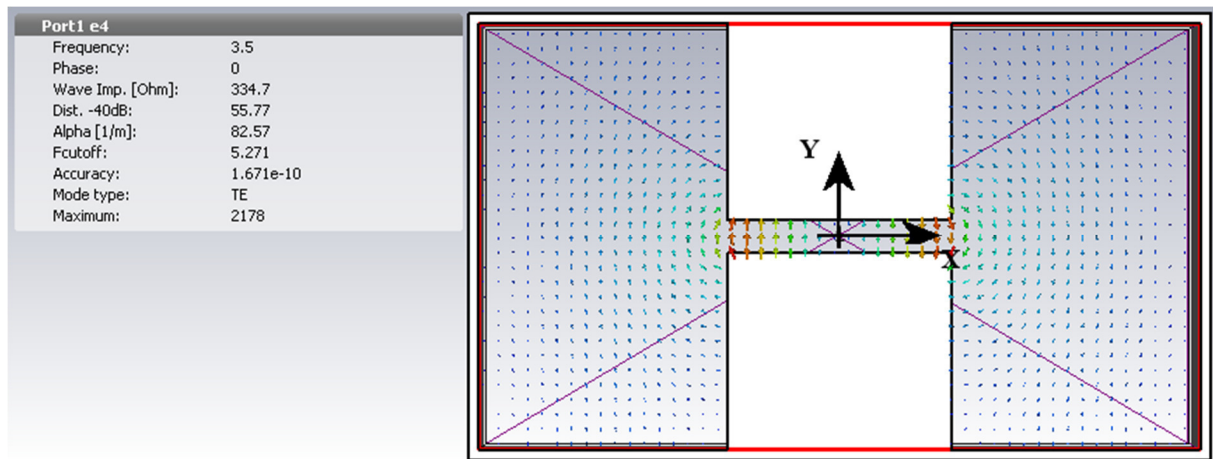


Figure 15: TE₂₀ with f_{cutoff} : 5.27GHz

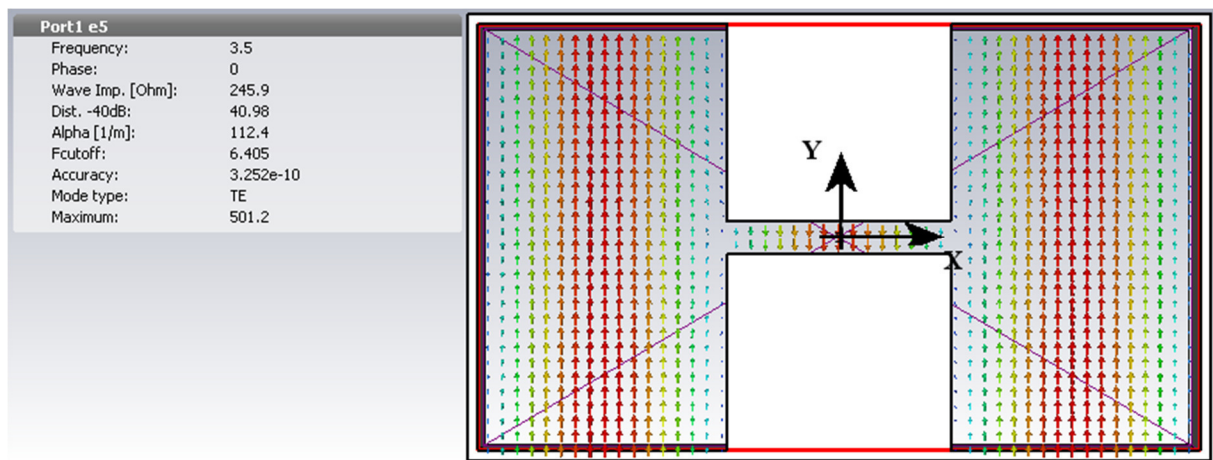


Figure 16: TE₃₀ with f_{cutoff} : 6.4GHz

4.1.2. Cavity back and connector

For the designed antenna a so-called short transition is chosen for easier implementation. This is a waveguide, which contains only rectangular shapes and edges, which is an advantage in design over types of where the sides are chamfered. It is implemented by adding b_r – height of the ridge inside of the cavity and k – depth of back chamber. As feedline a N-type-connector was selected. This embodiment is dimensioned and shown in figure 17 and 18.

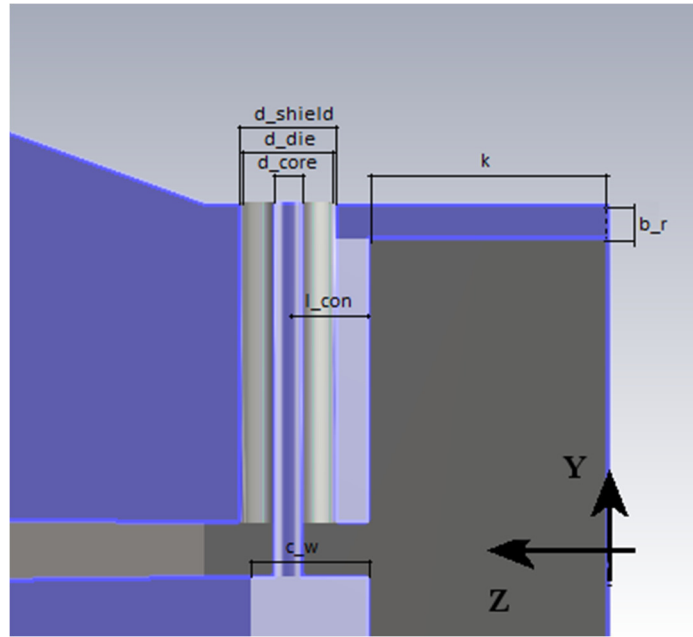


Figure 17: Cavity back

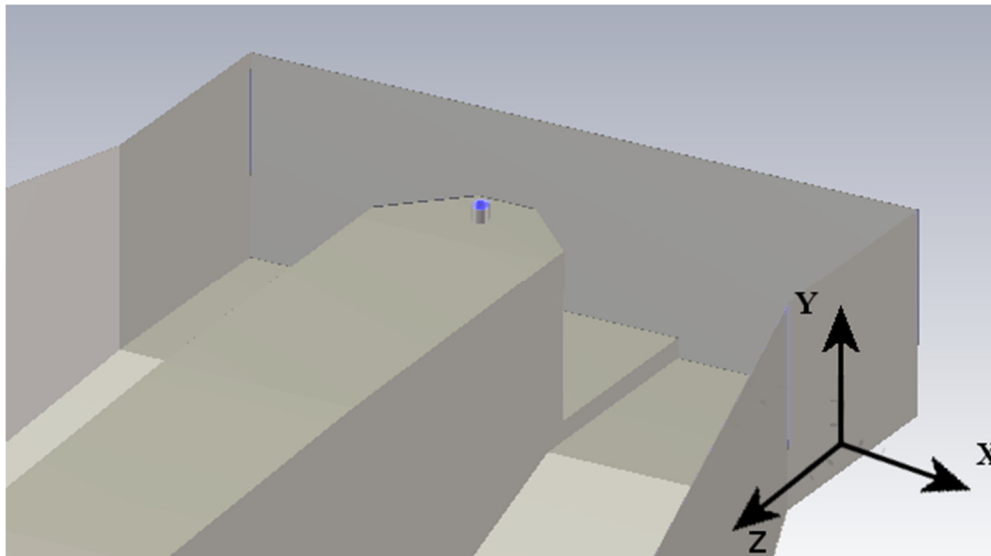


Figure 18: Horizontal cut

4.1.3. Horn

The dimensions of the aperture of the funnel antenna WA , H are calculated according to (20) and (21) for the desired gain of the antenna at a given frequency. This gain is required by 20 dB at the upper frequency limit of 6 GHz. This gain is achieved in a funnel without a ridge. First, the decibel value of the profile must be recalculated to absolute (45).

$$G = 10^{\frac{G_{[dB]}}{10}} = 10^{\frac{20}{10}} = 100, \quad (45)$$

$$WA = 0.489 \cdot \sqrt{G} \cdot \lambda = 0.489 \cdot \sqrt{100} \cdot 0.46 = 225 \text{ mm},$$

$$H = 0.332 \cdot \sqrt{G} \cdot \lambda = 0.332 \cdot \sqrt{100} \cdot 0.46 = 152 \text{ mm}.$$

From knowledge of wavelength, gain, width and aperture height and power supply dimensions the wavelength of the aperture L_h and the oblique radius of R_e and R_h according to (22) can be calculated (23), (24).

$$R_h = 0.0746 \cdot G \cdot \lambda = 0.0746 \cdot 100 \cdot 0,46 = 343 \text{ mm},$$

$$L_H = L_E = \frac{WA - a}{WA} \cdot \sqrt{R_h^2 - \frac{WA^2}{4}} = \frac{225 - 70}{225} \cdot \sqrt{343^2 - \frac{225^2}{4}} = 223 \text{ mm},$$

$$R_e = \frac{H}{H - b} \cdot \sqrt{L_h^2 - \frac{(H - b)^2}{4}} = \frac{152}{152 - 35} \cdot \sqrt{223^2 - \frac{(152 - 35)^2}{4}} = 166 \text{ mm}.$$

It is necessary to determine the constants ATL , PEL_h and PEL_e , where the PEL s are lost by phase errors, ATL is the attenuation of the waveguide and can be determined from the table in Annex T1. For calculation use the ATL table value listed in the literature [16].

$$ATL = 0.91 \text{ dB}.$$

To determine the phase error losses, the distribution values must first be calculated quadratic phase constants S_E for E-plane and S_H for H-plane according to (25) and (26).

$$S_E = \frac{H^2}{8 \cdot \lambda \cdot R_e} = \frac{152^2}{8 \cdot 46 \cdot 157} = 0.38,$$

$$S_H = \frac{WA^2}{8 \cdot \lambda \cdot R_h} = \frac{225^2}{8 \cdot 46 \cdot 343} = 0.4.$$

Using these values, we deduct from the table in Annex T1 the values for PEL_E and PEL_H :

$$PEL_E = 2.54,$$

$$PEL_H = 1.14.$$

The calculated current gain $G_{act} [dB]$ is according to (27):

$$G_{act[dB]} = 10 \log \left(\frac{4\pi \cdot H \cdot WA}{\lambda^2} \right) - ATL - PEL_H - PEL_E =$$

$$10 \log \left(\frac{4\pi \cdot 152 \cdot 225}{46^2} \right) - 0.91 - 1.14 - 2.54 = 18.5 \text{ dB} \triangleq G_{act} = 70.9.$$

The last calculation is then the calculation of the "new" gain G_{new} according to (28).

$$G_{new} = \frac{G_{req} \cdot G_d}{G_{act}} = \frac{100 \cdot 100}{70.9} = 141.$$

To find the optimal device dimensions the horn calculation will be recalculated several times like an iterative calculation with G_{new} . Second calculation:

$$WA = 0.489 \cdot \sqrt{G} \cdot \lambda = 0.489 \cdot \sqrt{141} \cdot 0.46 = 267 \text{ mm},$$

$$H = 0.332 \cdot \sqrt{G} \cdot \lambda = 0.332 \cdot \sqrt{141} \cdot 0.46 = 181 \text{ mm},$$

$$R_h = 0.0746 \cdot G \cdot \lambda = 0.0746 \cdot 141 \cdot 0.46 = 484 \text{ mm},$$

$$L_H = L_E = \frac{WA - a}{WA} \cdot \sqrt{R_h^2 - \frac{WA^2}{4}} = \frac{267 - 70}{267} \cdot \sqrt{484^2 - \frac{267^2}{4}} = 343 \text{ mm},$$

$$R_e = \frac{H}{H - b} \cdot \sqrt{L_h^2 - \frac{(H - b)^2}{4}} = \frac{181}{181 - 35} \cdot \sqrt{343^2 - \frac{(181 - 35)^2}{4}} = 270 \text{ mm},$$

$$S_E = \frac{H^2}{8 \cdot \lambda \cdot R_e} = \frac{181^2}{8 \cdot 46 \cdot 258} = 0.33,$$

$$S_H = \frac{WA^2}{8 \cdot \lambda \cdot R_h} = \frac{267^2}{8 \cdot 46 \cdot 484} = 0.4.$$

Using these values, we deduct from the table in Annex T1 new values for PEL_E and PEL_H :

$$PEL_E = 1.92,$$

$$PEL_H = 1.14,$$

$$G_{act[dB]} = 10 \log \left(\frac{4\pi \cdot H \cdot WA}{\lambda^2} \right) - ALT - PEL_H - PEL_E =$$

$$10 \log \left(\frac{4\pi \cdot 181 \cdot 267}{46^2} \right) - 0.91 - 1.14 - 1.92 = 20.6 \text{ dB} \triangleq G_{act} = 115,$$

$$G_{new} = \frac{G_{req} \cdot G_d}{G_{act}} = \frac{100 \cdot 141}{115} = 122.$$

Third iterative calculation:

$$WA = 0.489 \cdot \sqrt{G} \cdot \lambda = 0.489 \cdot \sqrt{122} \cdot 0.46 = 248 \text{ mm},$$

$$H = 0.332 \cdot \sqrt{G} \cdot \lambda = 0.332 \cdot \sqrt{122} \cdot 0.46 = 168 \text{ mm},$$

$$R_h = 0.0746 \cdot G \cdot \lambda = 0.0746 \cdot 122 \cdot 0.46 = 419 \text{ mm},$$

$$L_H = L_E = \frac{WA - a}{WA} \cdot \sqrt{R_h^2 - \frac{WA^2}{4}} = \frac{248 - 70}{248} \cdot \sqrt{419^2 - \frac{248^2}{4}} = 287 \text{ mm},$$

$$R_e = \frac{H}{H - b} \cdot \sqrt{L_h^2 - \frac{(H - b)^2}{4}} = \frac{168}{168 - 35} \cdot \sqrt{343^2 - \frac{(168 - 35)^2}{4}} = 222 \text{ mm},$$

$$S_E = \frac{H^2}{8 \cdot \lambda \cdot R_e} = \frac{168^2}{8 \cdot 46 \cdot 211} = 0.35,$$

$$S_H = \frac{WA^2}{8 \cdot \lambda \cdot R_h} = \frac{248^2}{8 \cdot 46 \cdot 419} = 0.4.$$

Using these values, we deduct from the table in Annex T1 new values for PEL_E and PEL_H :

$$PEL_E = 1.92,$$

$$PEL_H = 1.14.$$

The calculated current gain $G_{act} [dB]$ is according to (27):

$$G_{act[dB]} = 10 \log \left(\frac{4\pi \cdot H \cdot WA}{\lambda^2} \right) - ALT - PEL_H - PEL_E =$$

$$10 \log \left(\frac{4\pi \cdot 168 \cdot 248}{46^2} \right) - 0.91 - 1.14 - 1.92 = 20 \text{ dB}.$$

The aim of 20 dB for the horn dimensions is reached after the third iteration.

4.1.4. Ridges

The last part is to calculate the ridged. The ridge profile is described by the equation (29), where k is the constant (equation (30)) which is calculated for the proposed antenna:

$$k = \frac{1}{L} \cdot \ln\left(\frac{z(L)}{z(0)}\right) = \frac{1}{287} \cdot \ln\left(\frac{84}{1.57}\right) = 0.013867 \text{mm}^{-1}.$$

By using the calculated values of $z(y)$, it's the half distance between the ridges at y it is easy to design the form of the ridges (Tab. 2).

y [mm]	$z(y)$ [mm]	y [mm]	$z(y)$ [mm]	y [mm]	$z(y)$ [mm]
0	1.57	$L \cdot 11/16 = 197.3$	24.2	$L \cdot 15/16 = 269.1$	65.5
$L \cdot 1/8 = 35.9$	2.6	$L \cdot 6/8 = 215.3$	31.1	$L \cdot 31/32 = 278.0$	74.2
$L \cdot 2/8 = 71.8$	4.3	$L \cdot 19/24 = 227.2$	36.7	$L \cdot 63/64 = 282.0$	78.9
$L \cdot 3/8 = 107.6$	7	$L \cdot 5/6 = 239.2$	43.3	$L \cdot 127/128 = 284.8$	81.4
$L \cdot 4/8 = 143.5$	11.5	$L \cdot 7/8 = 251.1$	51.1	$L = 287.0$	84.0
$L \cdot 5/8 = 179.4$	18.9	$L \cdot 29/32 = 278$	57.8		

Table 2: The $z(y)$ function values describe the shape of the ridge

It's possible to construct the ridges with an exponential formula, this would rise the complication of optimization of all other parameters. With the division of the ridges into 16 parts, each with dependencies on other parameters, the possibility of performing an automatic optimization by CST MWS is made easier.

4.2. Log-periodic antenna calculation

To one of the half antenna a rectangular bar is added to improve the mechanical stability. The bar has a hole which is used to put through the feeding cable. In order to simplify the production, the thickness of the sheet was predetermined to $b = 2 \text{ mm}$.

In the first step τ , σ and the characteristic input impedance will be chosen between the recommended limits.

$$\tau = 0.885,$$

$$\sigma = 0.115,$$

$$R_0 = 50\Omega.$$

With $f_n = 6$ GHz, $f_l = 1$ GHz and the middle distance $s = 20$ all parameters mentioned in 3.4. will be calculated with the equations (31) to (37), (39) and (41) to (44):

$$\alpha_{rad} = \arctan \frac{1 - \tau}{4 \cdot \sigma} = \arctan \frac{1 - 0.885}{4 \cdot 0.115} = 0.24,$$

$$\alpha = \alpha_{rad} \cdot \frac{180^\circ}{\pi} = 0.24 \cdot \frac{180^\circ}{\pi} = 14.0^\circ,$$

$$B = \frac{f_n}{f_l} = \frac{6 \text{ GHz}}{1 \text{ GHz}} = 6,$$

$$B_{ar} = 1.1 + 30.8 \cdot (1 - \tau) \cdot \sigma = 1.1 + 30.8 \cdot (1 - 0.885) \cdot 0.115 = 1.51,$$

$$B_s = B \cdot B_{ar} = 6 \cdot 1.15 = 9.0,$$

$$N = 1 + \frac{\log(B_s)}{\log\left(\frac{1}{\tau}\right)} = 1 + \frac{\log(9)}{\log\left(\frac{1}{0.885}\right)} = 19,$$

$$L_1 \approx \frac{c}{2 \cdot f_l} = \frac{\lambda_{max}}{2} = \frac{3 \cdot 10^8}{2 \cdot 1 \cdot 10^9} = 150 \text{ mm},$$

$$L_{total} = \sum_{i=1}^n L_i = 1.183 \text{ m},$$

$$d_1 = 2 \cdot \sigma \cdot L_1 = 2 \cdot 0.115 \cdot 150 \text{ mm} = 34.5 \text{ mm},$$

$$a_1 = \frac{L_1}{s} = \frac{150 \text{ mm}}{20} = 7.5 \text{ mm},$$

$$L = \sum_{i=1}^{n-1} d_i = 271 \text{ mm},$$

$$l_{stub} = \frac{\lambda_{max}}{8} = \frac{300 \text{ mm}}{8} = 37.5 \text{ mm}.$$

5. Simulation and optimization

Antennas of this thesis were simulated with CST MWS, whose simulation tools are used in leading industries across fields such as automotive, aerospace, communication, defense, electronics, energy and healthcare, in order to design, analyze and optimize performance, reliability electromagnetic compatibility and signal/power integrity. CST MSW offers solvers for the whole spectrum from statics up to optical frequencies, as well as multiphysics solvers for thermal, mechanical and particle effects [2].

5.1. CST MWS Time domain solver

A time domain solver calculates the development of fields through time at discrete locations and at discrete time samples. It calculates the transmission of energy between various ports or other excitation sources. Consequently, a time domain solver is remarkably efficient for most high frequency applications such as connectors, transmission lines, filters, antennas etc. and can obtain the entire broadband frequency behavior of the simulated device from a single calculation run.

In CST MWS two time domain solvers are available. The Transient solver, which is based on the Finite Integration Technique (FIT), was used for simulation. The Transient solver applies some highly advanced numerical techniques. This allows a very memory efficient computation together with a robust hexahedral meshing to successfully simulate extremely complex structures. The fields are calculated step by step through time by the Leap-Frog updating scheme, an explicit update formulation for the loss-free case of the discretized set of Maxwell's Grid Equations.

5.2. Finite Integration Technique (FIT) – Maxwell equations

FIT is first proposed by Weiland in 1976/1977, this numerical method provides a universal spatial discretization scheme applicable to various electromagnetic problems ranging from static field calculations to high frequency applications in time or frequency domain. FIT discretizes the following integral form of Maxwell's equations rather than the differential one.

The Maxwell equations describe not only the formation but also the interaction from electric and magnetic fields, and how electric charges and electric currents act as sources for these. All the field simulation programs base their calculations on the following equations: Ampere's law, Faraday's law of induction, Gauss's law for electricity and Gauss's law for magnetism.

Ampere's law relates magnetic fields to electric currents. Using this law, it is possible to determine the magnetic field associated with a given current, or the current associated with a given magnetic field. It states that the line integral of the magnetic field around a closed loop is proportional to the electric current flowing through the loop. [20]

$$\oint_{\partial A} \vec{H} \cdot d\vec{s} = \int_A \left(\frac{\partial \vec{D}}{\partial t} + \vec{j} \right) \cdot d\vec{A}. \quad (46)$$

The Faraday law states that a change of the magnetic field \vec{B} on an area dA over a time dt , induces an electric field \vec{E} .

$$\oint_{\partial A} \vec{E} \cdot d\vec{s} = - \int_A \frac{\partial \vec{B}}{\partial t} \cdot d\vec{A}. \quad (47)$$

Gauss's law for electricity gives a connection between the divergence of the displacement density \vec{D} and the charge density ρ . The electric flux out of any closed surface is proportional to the total charge enclosed within the surface.

$$\oint_{\partial V} \vec{D} \cdot d\vec{A} = \int_V \rho \cdot dV. \quad (48)$$

Gauss's law for magnetism says that the magnetic flux from any closed surface is equal to zero when the magnetic field does not have a source.

$$\oint_{\partial V} \vec{B} \cdot d\vec{A} = 0. \quad (49)$$

5.3. Signals in time domain simulation

The time domain solver calculates the development of fields through time at discrete locations and at discrete time samples. Every structure must have at least one port where the fields can propagate into or out of the structure. At these ports, voltages and currents are monitored that are the input and output signals of the structure.

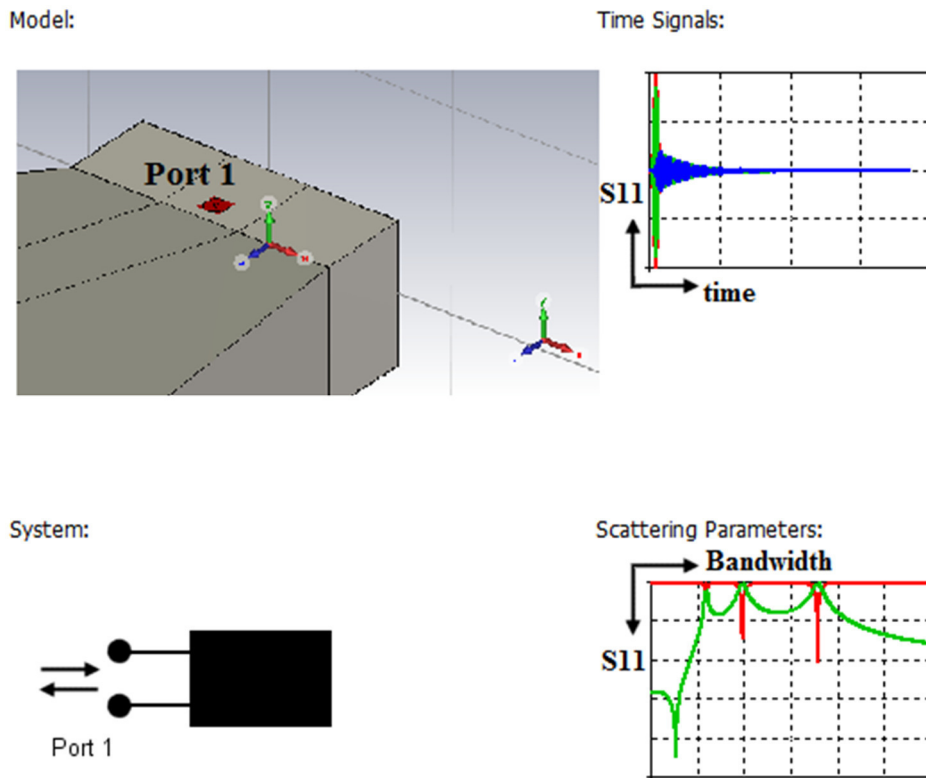


Figure 19: Function of signals in time domain solver

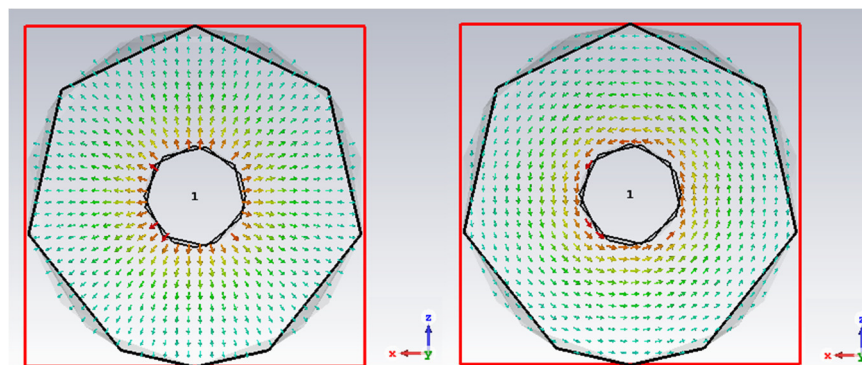


Figure 20: Port distribution E-field (left) and H-field (right)

According to these signals, the transfer functions of the structure are calculated. At this stage, the structure can be considered as an abstract system with input and output signals that are related by the calculated transfer functions, in our case the scattering parameter (S-parameter).

5.4. CST MWS settings

For the simulation the preinstalled template for antennas, waveguide was selected. The Time Domain solver with Dimensions: mm and Frequency: GHz. Lowest frequency is 0.5 GHz and 6.5 GHz maximum with farfield monitors for 1 GHz, 3.5 GHz and 6 GHz. Background material is 'normal', all boundaries are opened with space and no symmetry was chosen.

5.5. Mesh

The term mesh is assigned to a geometry that is broken up into discrete number of elements. Several types of mesh can be considered. It all depends on what the researcher selects for meshing method. The following image shows the DRHA mesh view. Tiny or critical parts like the input area are split into smaller mesh cells.

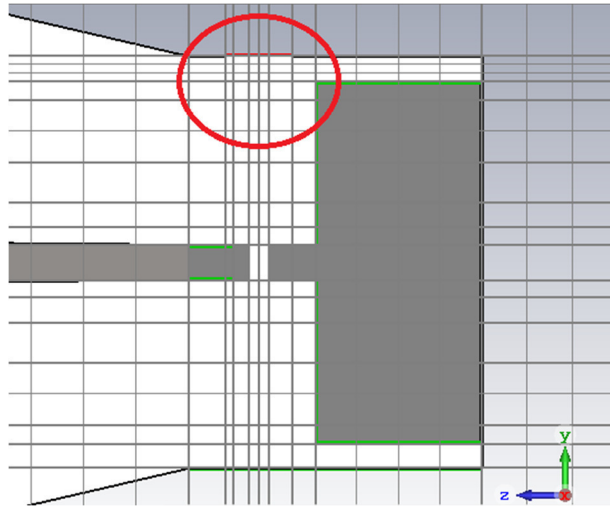


Figure 21: Mesh cells of DRHA

To get a more precise solution a very high mesh cell value was selected: DRHA has 2.050.464 and LPDA 558.620 mesh cells. Hexahedral mesh type has for both simulations an accuracy of -40 dB.

5.6. Double ridged horn antenna

5.6.1. Parameter overview and optimization

In the following table you will find all parameters necessary to design the calculated DRHA. To find the best solution for S_{11} all parameters with a '*' were optimized by CST MWS Parameter Sweep.

parameter	dimension [mm]	description
a	70	width of the waveguide
b	35	height of the waveguide
l_{wave}	25	length of the waveguide
d^*	3	the gap between the ridges
s	21	width of the ridges
WA	248	width of the Horn
H	168	height of the Horn
L	287	length of the Horn
$a_{r=s}$	21	width of the ridges inside cavity back
b_{r^*}	2	height of the ridges inside cavity back
c_{w^*}	7	length of chamfer edges of the ridges
c_{angle}	45°	angle of chamfer edges of the ridges
l_{con^*}	6	distance between end of the back chamber and the connector
d_{die}	5.7	diameter of the dielectric of the connector
d_{core}	1.7	diameter of the core of the connector
d_{shield}	5.735	diameter of the shield of the connector

Table 3: DRHA parameter overview

Attached (A2) are for every optimized parameter some Parameter Sweep results. As you can see the program simulates every time with a new value the whole antenna function. By finding the best S_{11} result, the optimization goes to the next parameter. The final S_{11} parameter is slightly worse because a very high accuracy (5 million mesh cells) was selected for the final simulation.

5.6.2. Simulation results of DRHA

The final version of antenna is shown below in Figure 22 and 23.

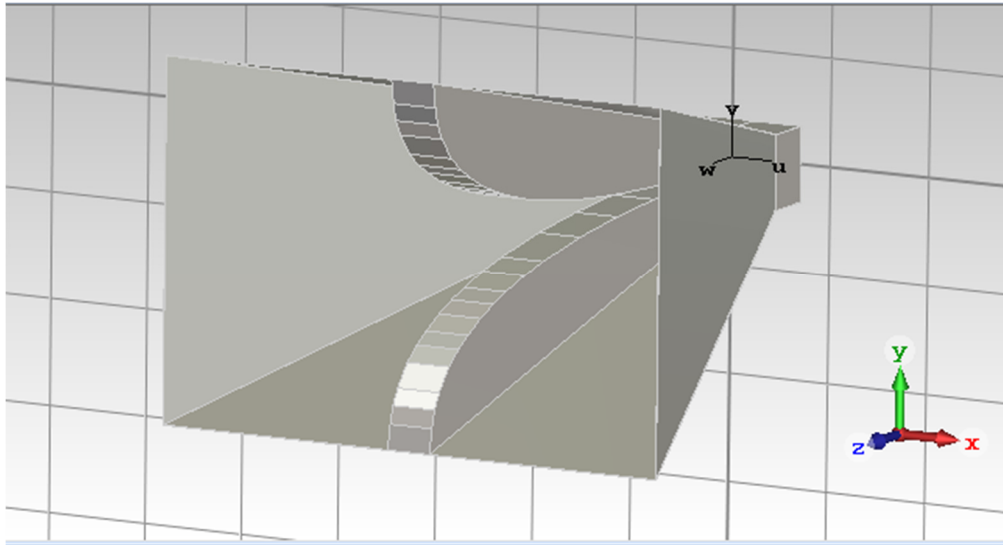


Figure 22: DRHA 3D view

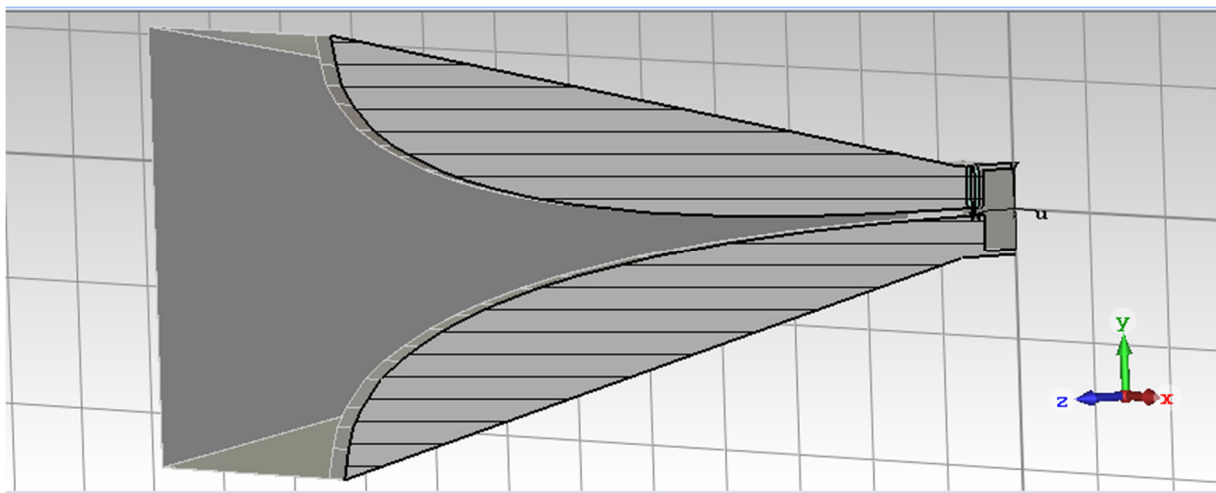


Figure 23: DRHA 3D vertical cut view

Only small changes in the area of the cavity back were necessary to meet the requirements. In the range of 1 GHz to 6 GHz the S_{11} parameter and thus VSWR has superb results with only small vibes (Fig. 24 and Fig. 25).

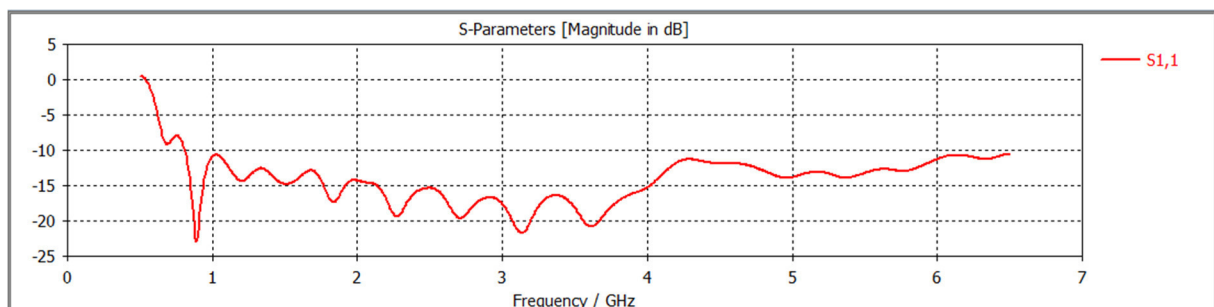


Figure 24: DRGA final S_{11} -parameter

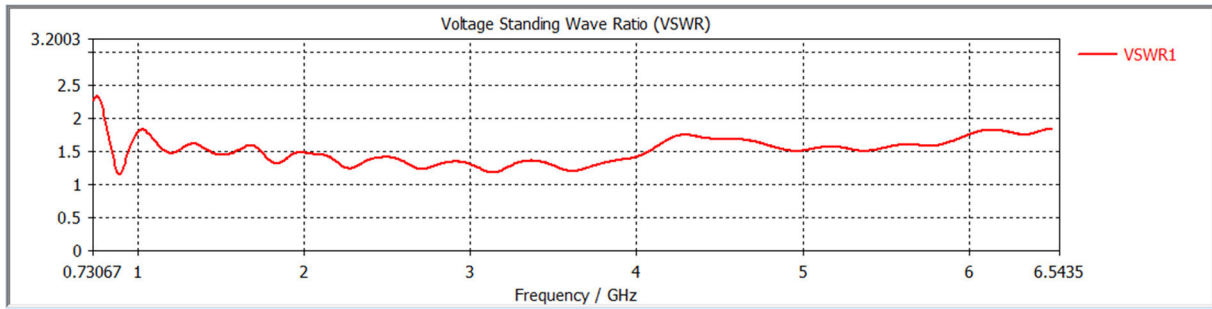


Figure 25: DRHA final VSWR-parameter

5.7. Log-periodic dipole antenna

5.7.1. Parameter overview and optimization

The calculated values are used as basic construction. Since the S_{11} result is very bad (Figure 26) some optimization must be done. The goal is to move the graph below -10 dB.

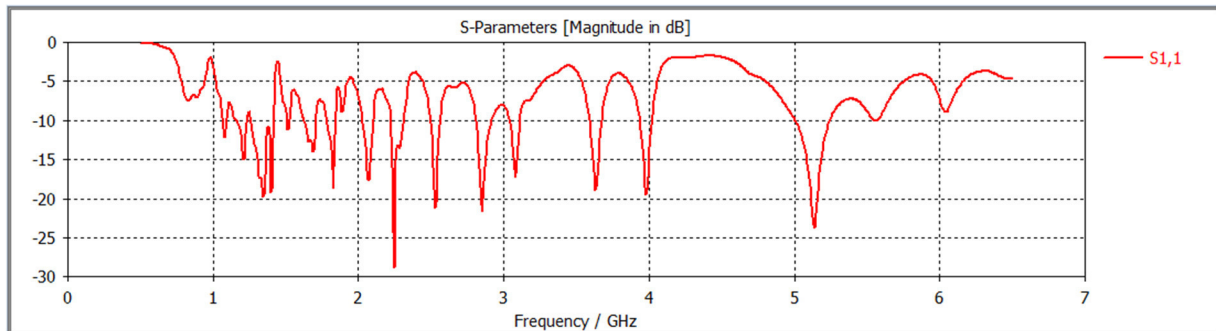


Figure 26: S_{11} of calculated design

Beginning with the middle distance s between the beams (Fig. 27). By using a smaller value for s the graph is going step by step down. Because of visual reasons only three graphs are shown below. Best result for further optimization is $s = 10$ mm.

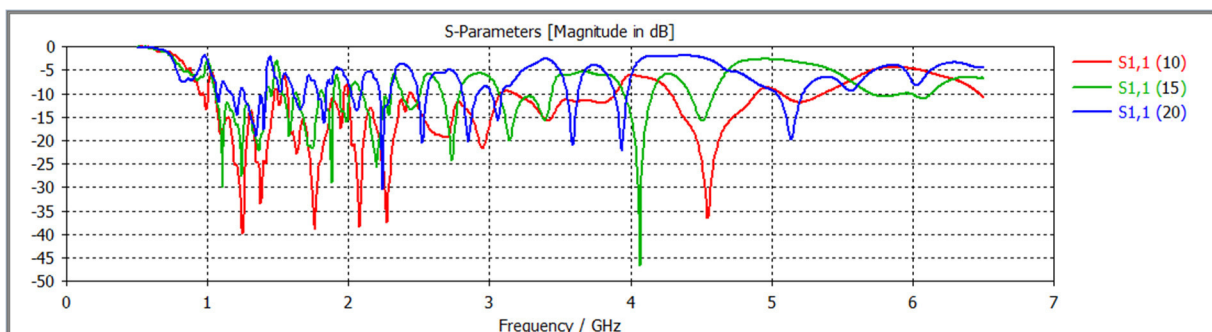


Figure 27: Different s -values

By changing the length of the terminating stub it's possible to modify the S_{11} parameter between lower frequencies (Fig. 28). With a length of $L_{stub} = 19$ mm S_{11} is in the range of 1 to 3 GHz almost below -10 dB.

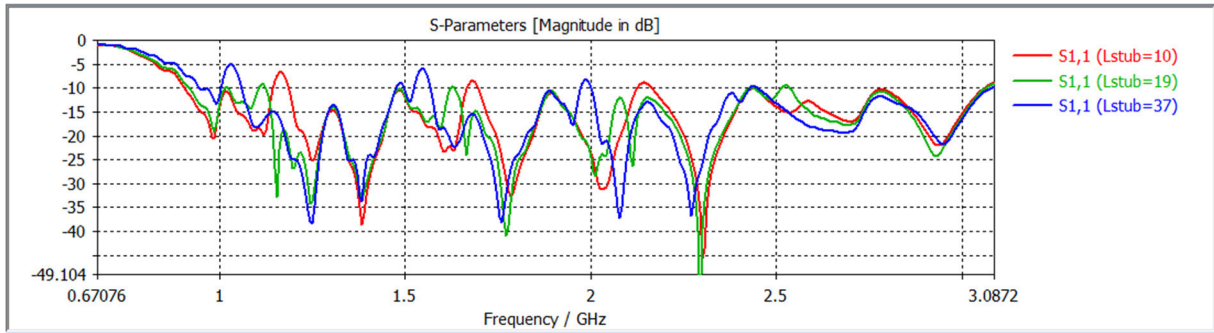


Figure 28: Different Lstub-values

The last of the ‘simple’ optimization parameter is d . The distance between the sheets has an immense influence to S_{11} (Fig. 29). After choosing $d = 3$ mm there is one last arc left (Arrow in Fig. 30) to optimize.

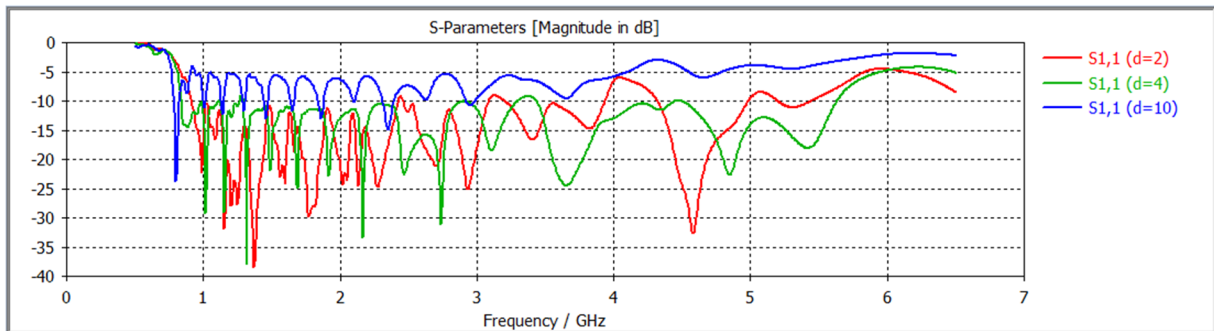


Figure 29: Different d -values

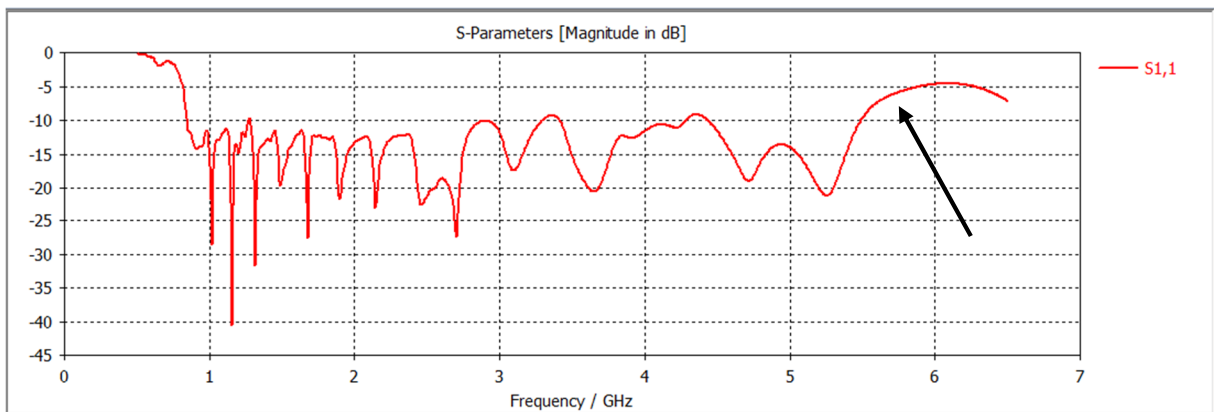


Figure 30: S_{11} after ‘simple’ optimization

As known long beams are for low frequencies responsible and shorter ones for higher frequencies. By experimenting with diameters and distances of the shorter beams the following result is obtained (Fig. 31).

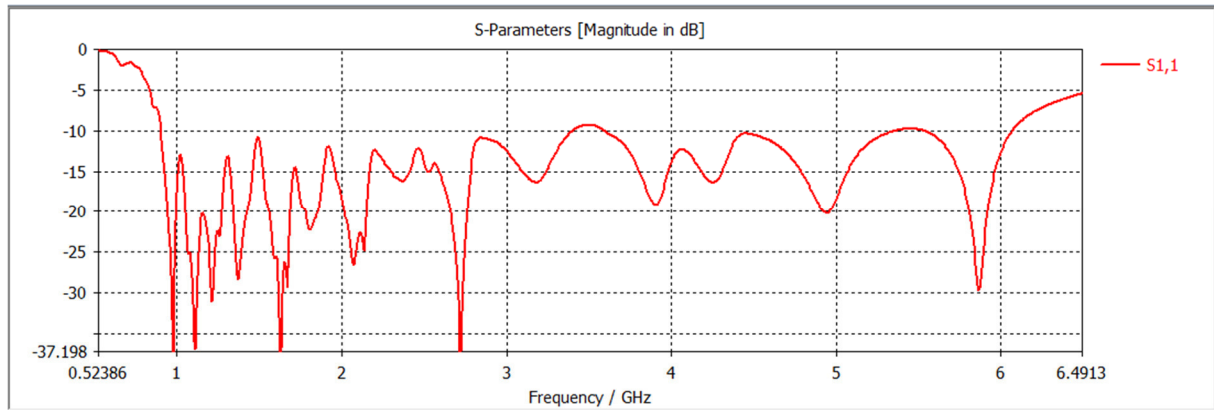


Figure 31: Different a_n - and d_n -values

In the following table you will find all parameters necessary to design the calculated LPDA. To find the best solution for S_{11} all parameters with a ‘*’ were optimized by CST MWS Parameter Sweep.

L_n	value	d_n	value	a_n	value	parameter	Value
L_1	150 mm	$d_{1,2}$	35 mm	a_1	7.5 mm	s^*	10 mm
L_2	133 mm	$d_{2,3}$	31 mm	a_2	6.5 mm	L_{stub}^*	19 mm
L_3	117 mm	$d_{3,4}$	27 mm	a_3	6 mm	d^*	3 mm
L_4	104 mm	$d_{4,5}$	24 mm	a_4	5 mm	b	2 mm
L_5	92 mm	$d_{5,6}$	21 mm	a_5	4.5 mm	d_{core}	1.7 mm
L_6	81 mm	$d_{6,7}$	19 mm	a_6	4 mm	d_{die}	5.7 mm
L_7	72 mm	$d_{7,8}$	17 mm	a_7	3.5 mm	d_{shield}	5.735 mm
L_8	64 mm	$d_{8,9}$	15 mm	a_8	3 mm		
L_9	56 mm	$d_{9,10}$	13 mm	a_9	3 mm		
L_{10}	50 mm	$d_{10,11}$	12 mm	a_{10}	2.5 mm		
L_{11}	44 mm	$d_{11,12}$	10 mm	a_{11}	2 mm		
L_{12}	39 mm	$d_{12,13}$	9 mm	a_{12}	2 mm		
L_{13}	35 mm	$d_{13,14}^*$	6 mm	a_{13}	2 mm		
L_{14}	31 mm	$d_{14,15}$	7 mm	a_{14}^*	1 mm		
L_{15}	27 mm	$d_{15,16}^*$	3 mm	a_{15}^*	1 mm		
L_{16}	24 mm	$d_{16,17}$	6 mm	a_{16}^*	6 mm		
L_{17}	21 mm	$d_{17,18}^*$	3 mm	a_{17}	1 mm		
L_{18}	19 mm	$d_{18,19}^*$	2 mm	a_{18}	1 mm		
L_{19}	17 mm			a_{19}	1 mm		

Table 4: LPDA parameter overview

5.7.2 Simulation results of LPDA

The design (Fig. 32) and production of this antenna is very simple. It's only required to emboss a sheet of metal and add for the mechanic stable two beams. To meet the requirements changes at the beginning and the end of antenna were required. Final results of the simulation are shown below.

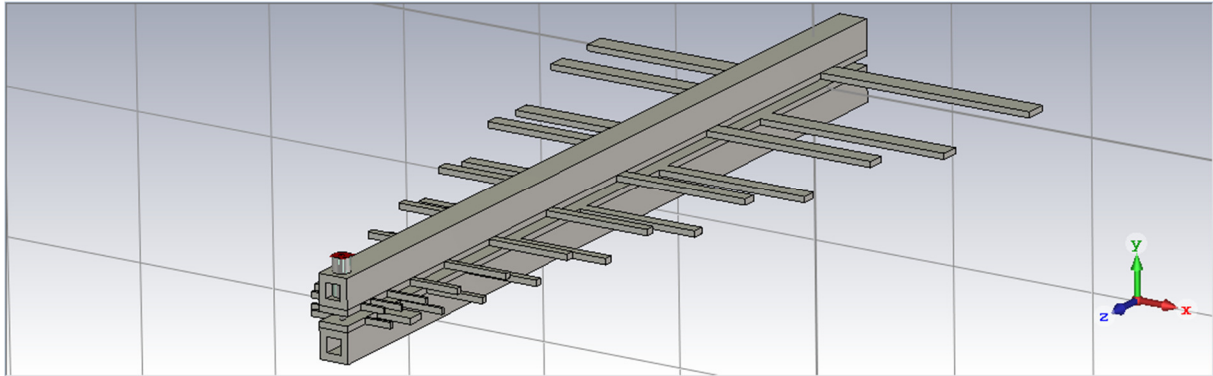


Figure 32: LPDA 3D view

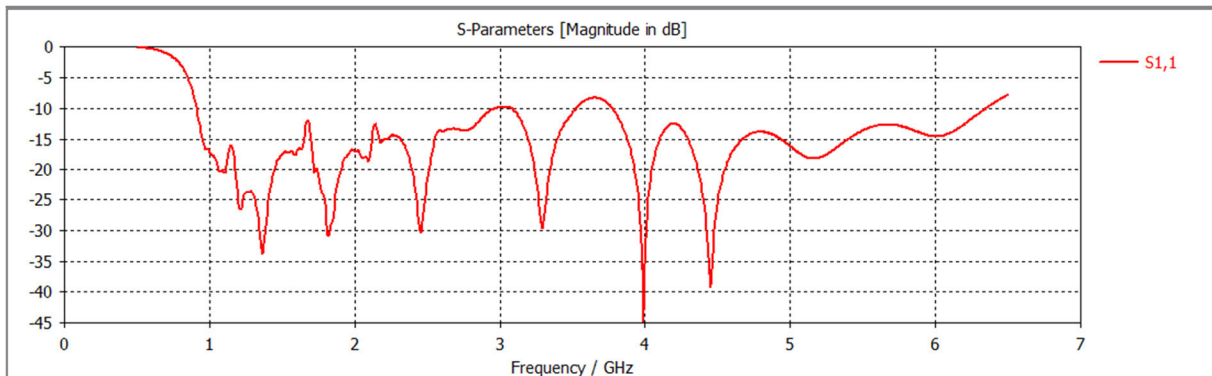


Figure 33: LPDA final S₁₁-parameter

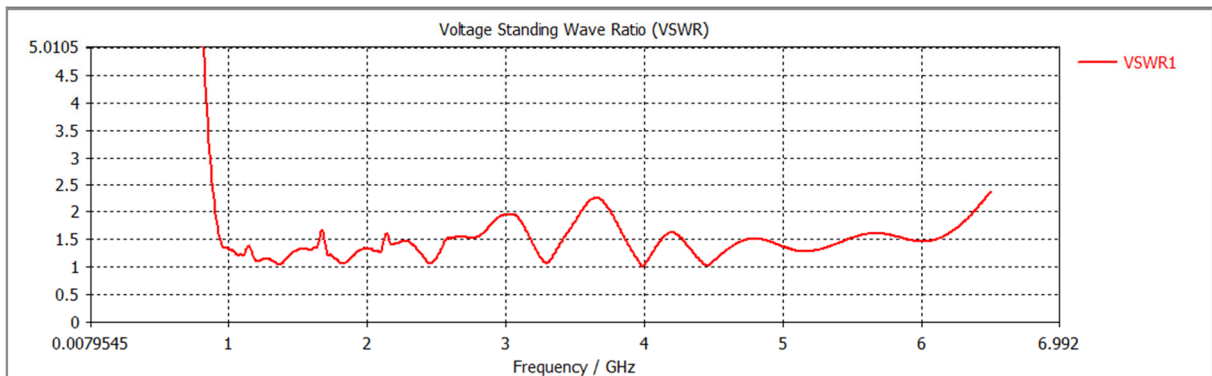


Figure 34: LPDA final VSWR-parameter

6. Conclusion and further work

Since 1886, the birth of wireless technology, many different antennas have been developed for any application. In this thesis a very simple (Log-per dipole antenna) and a more modern (Double ridged horn antenna) antenna was simulated and compared.

Thanks to the simulation with programs like CST MWS, it is possible to design and prove any antenna. This process is made easier by different systematical methods that allow to get great results at the end. It was crucial to maintain an order in the optimizations of each component. The antennas designed in this thesis possesses a low VSWR across its operational frequency band. It has a high and uniform gain and radiation pattern with a very low reflection factor.

Its bandwidth from 1 GHz to 6 GHz meets the requirements set by the university, and some of its characteristics exceeded the expectations. The gain of the DRHA at an upper limit frequency of 20 dB only applies to the funnel antenna without an inserted ridge. When inserting the ridge, this gain at the upper limit frequency will fall.

The advantages and disadvantages of the antennas are shown below:

DRHA	
Advantage	Disadvantage
<ul style="list-style-type: none"> - Good performance – low reflection - More directional - Wide Band - More options to improve the gain 	<ul style="list-style-type: none"> - Time consuming construction and production - Expensive manufacture
LPDA	
Advantage	Disadvantage
<ul style="list-style-type: none"> - Simple construction and production - Cheap manufacture - Feed point impedance mostly constant - Easy so increase bandwidth with adding elements. 	<ul style="list-style-type: none"> - Very low gain - VSWR depending on size

Table 5: DRHA, LPDA advantages and disadvantages

The output of the diploma thesis is a simulated DRHA and LPDA whose were made according to the requirements they meet, its working band is 1 GHz up to 6 GHz in which the reflection coefficient S_{11} is $< -10 \text{ dB}$. In the future, the production of both antennas will be needed to test their functionality in practice. The technical drawings are attached thus the antennas are ready to manufacture.

By comparing them there are different views. From the point of view of cost and production, it is more economical to use an LPDA. The requirements are fulfilled just like at the DRHA. From the point of view of quality, it is advisable to use a DRHA. During the simulation, various optimization options are already available. For example, by rounding off the ridges at the end or by a more complex cavity back better simulation results are achievable.

7. References

- [1] rnelectronics.com, EMC testing. [online]. [Accessed 30 January 2018]. Available from: www.rnelectronics.com/testing-services/emc-testing.html#our-emc-testing-capabilities
- [2] cst.com, CST MWS. [online]. [Accessed 30 January 2018]. Available from: www.cst.com/products/cstmws
- [3] schwarzbeck.de, Double-Ridged Horn Antennas. [online]. [Accessed 30 January 2018]. Available from: www.schwarzbeck.de/en/antennas/broadband-horn-antennas/double-ridged-horn-antenna.html
- [4] amateur-radio-antenna.com, Log.-Periodic Antenna LPDA/115-1000. [online]. [Accessed 30 January 2018]. Available from: www.amateur-radio-antenna.com/emc-antenna/log-periodic-antenna-lpda-115-1000.php
- [5] searchmobilecomputing.techtarget.com, antenna. [online]. [Accessed 30 January 2018]. Available from: <http://searchmobilecomputing.techtarget.com/definition/antenna>
- [6] tutorialspoint.com, Antenna Theory – Types of Antennas. [online]. [Accessed 30 January 2018]. Available from: www.tutorialspoint.com/antenna_theory/antenna_theory_types_of_antennas.htm
- [7] tutorialspoint.com, Antenna Theory – Basic Parameters. [online]. [Accessed 30 January 2018]. Available from: www.tutorialspoint.com/antenna_theory/antenna_theory_basic_parameters.htm
- [8] Constantine, A. Balanis. Antenna Theory. New Jersey : John Wiley & Sons, 2005. [online]. [Accessed 30 January 2018]. Available from: nashvillelibrary.dyndns.org:823/YourFreeLibrary/Antennas/Antenna%20Theory%20Design.pdf
- [9] Johnson, Richard C. Antenna Engineering Handbook. Atlanta, Georgia : R. R. Donnelley & Sons Company ,1993.

- [10] tutorialspoint.com, Antenna Theory – Radiation Pattern. [online]. [Accessed 30 January 2018]. Available from: www.tutorialspoint.com/antenna_theory/antenna_theory_radiation_pattern.htm
- [11] Avionics Department. Electronic Warfare and Radar Systems Engineering Handbook. POINT MUGU : Technical Communication Office, 2013. [online]. [Accessed 30 January 2018]. Available from: www.phys.hawaii.edu/~anita/new/papers/militaryHandbook/waveguid.pdf
- [12] Pozar, David M. Microwave Engineering. 2012, John Wiley & Sons
Chapter 3, Introduction
- [13] Straw, R. Dean. The ARRL Antenna Book 21st, Newington : ARRL, 2007.
Chapter 10-2
- [14] Lo, Y. T. Antenna Handbook. Illinois : Springer, Boston, MA, 2005,
Chapter 13, p. 739
- [15] Hoefler, W. J. R. Closed Form Expressions for the Parameters of Finned and Ridged Waveguides. IEEE TRANSACTIONS ON MICROWAVE THEORY AND TECHNIQUES, VOL. MT’F30, NO. 12, 1982.
- [16] MILIGAN, T., A. Modern Antenna Design. New Jersey: John Willey & Sons, 2005.
chapter 7.1.2
- [17] Ghorbani, M. Khaleghi A. Double Ridged Horn Antenna Designs for Wideband Applications. Tehran, Iran : IEEE, 2011. [online]. [Accessed 30 January 2018]. Available from: <http://ieeexplore.ieee.org/document/5955679/>
- [18] MILIGAN, T. A. Modern Antenna Design. New Jersey: John Willey & Sons, 2005.
chapter 7.6
- [19] MILIGAN, T., A. Modern Antenna Design. New Jersey: John Willey & Sons, 2005.
chapter 11.12
- [20] CST Studio Suite 2017, Online Help, Signals in Time Domain Simulations

- [21] itwissen.info, S-Parameter (Streuparameter). [online]. [Accessed 30 January 2018]. Available from: <http://www.itwissen.info/Streuparameter-S-Parameter-scattering-parameter.html>

V. List of Annexes

A1: Table for determination of PEL_H and PEL_E	43
A2: Optimization of DRHA	44
A3: Characteristic of DRHA	46
A4: Characteristic of LPDA	49
A5: Technical drawing DRHA	52
A6: Technical drawing LPDA	54

A1. Table for determination of PEL_H and PEL_E

S_H, S_E	Uniform PEL_E	Cosine PEL_H
0.05	0.04	0.02
0.1	0.15	0.07
0.15	0.34	0.16
0.2	0.62	0.29
0.25	0.97	0.45
0.3	1.40	0.65
0.35	1.92	0.88
0.4	2.54	1.14
0.45	3.24	1.43
0.5	4.04	1.75
0.55	4.93	2.09
0.6	5.91	2.44
0.65	6.69	2.82
0.7	8.04	3.20
0.75	9.08	3.58
0.8	9.98	3.95
0.85	10.60	4.31
0.9	10.87	4.65

A2. Optimization of DRHA

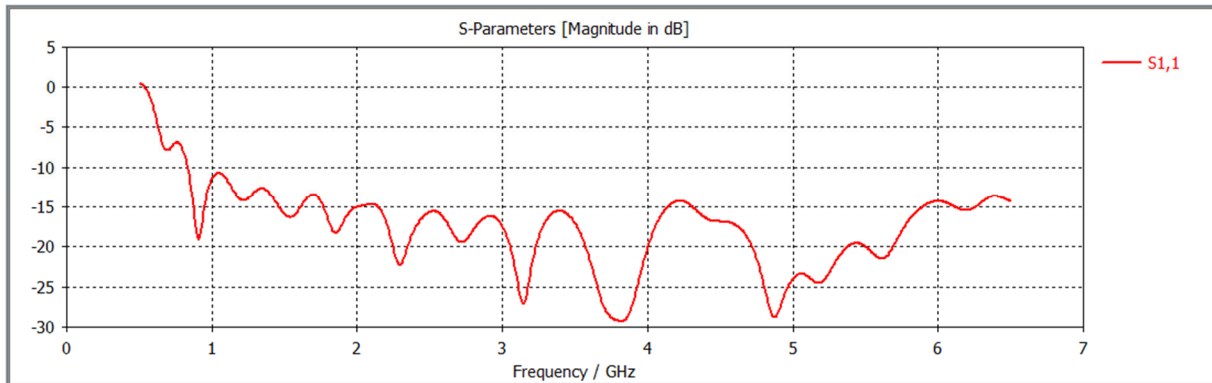


Figure 35: Calculated result of DRHA

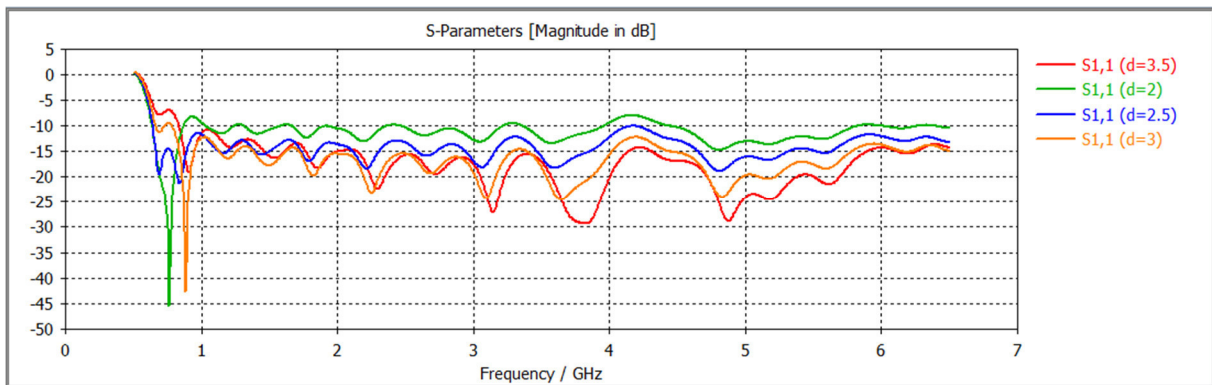


Figure 36: Different d for DRHA

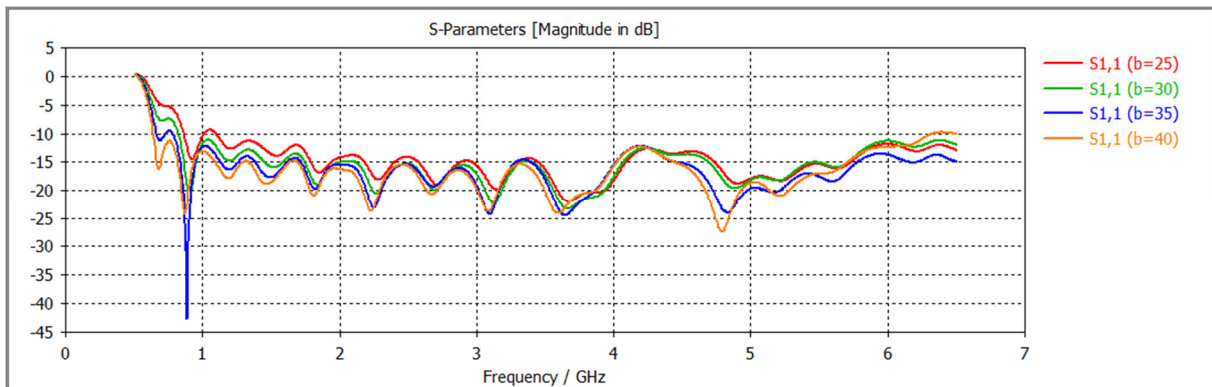


Figure 37: Different b for DRHA

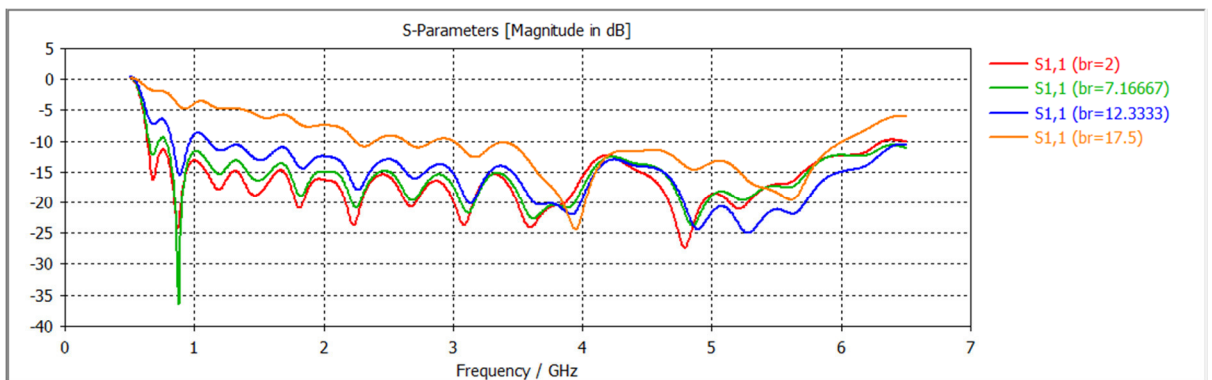


Figure 38: Different b_r for DRHA

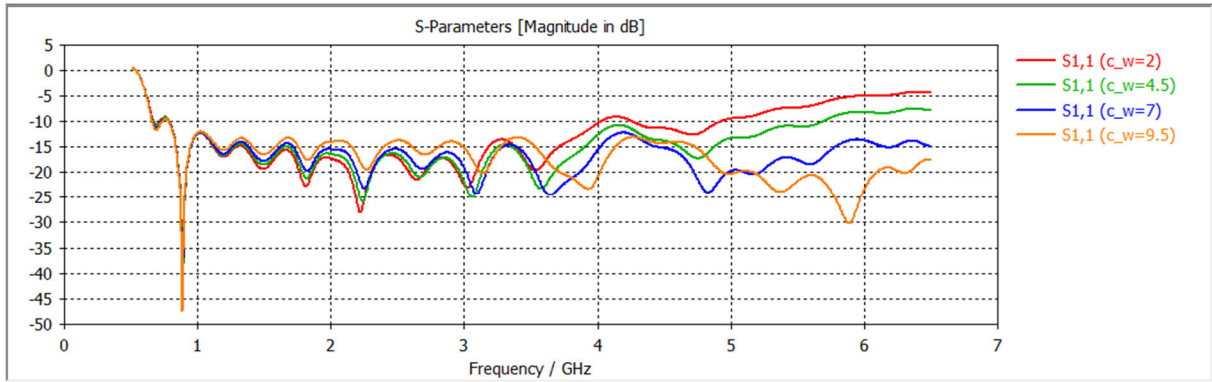


Figure 39: Different c_w for DRHA

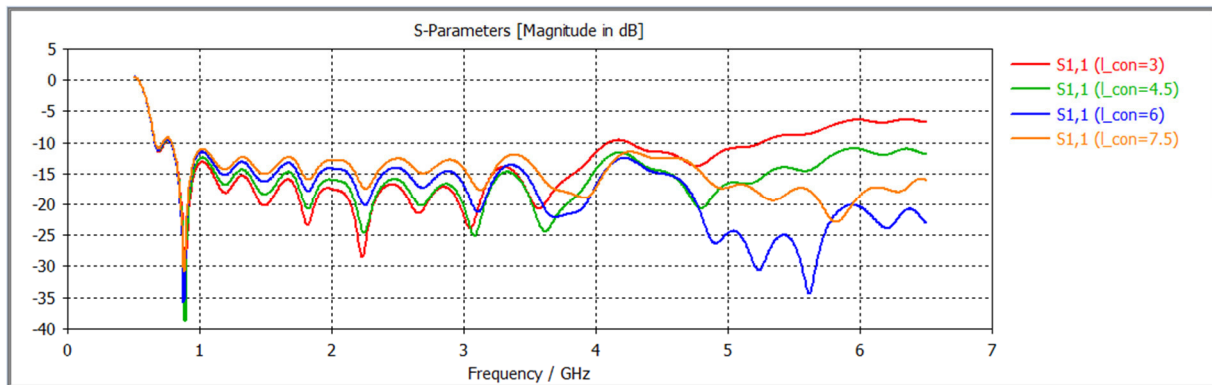


Figure 40: Different l_{con} for DRHA

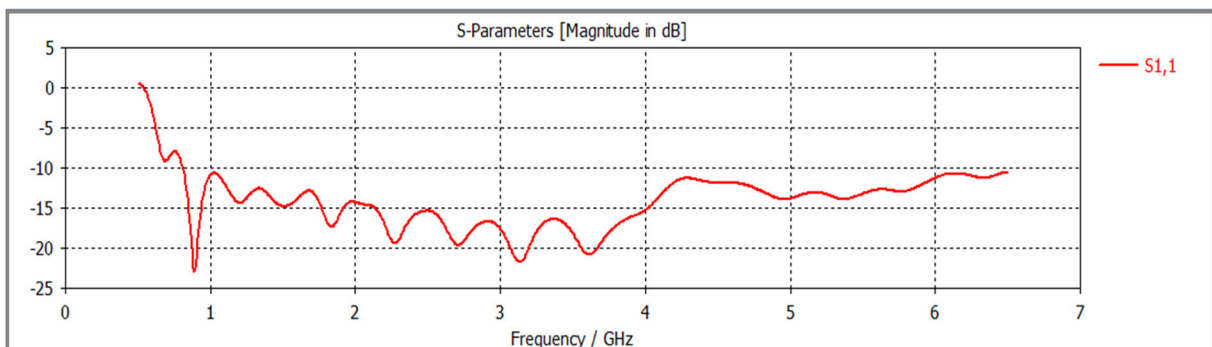
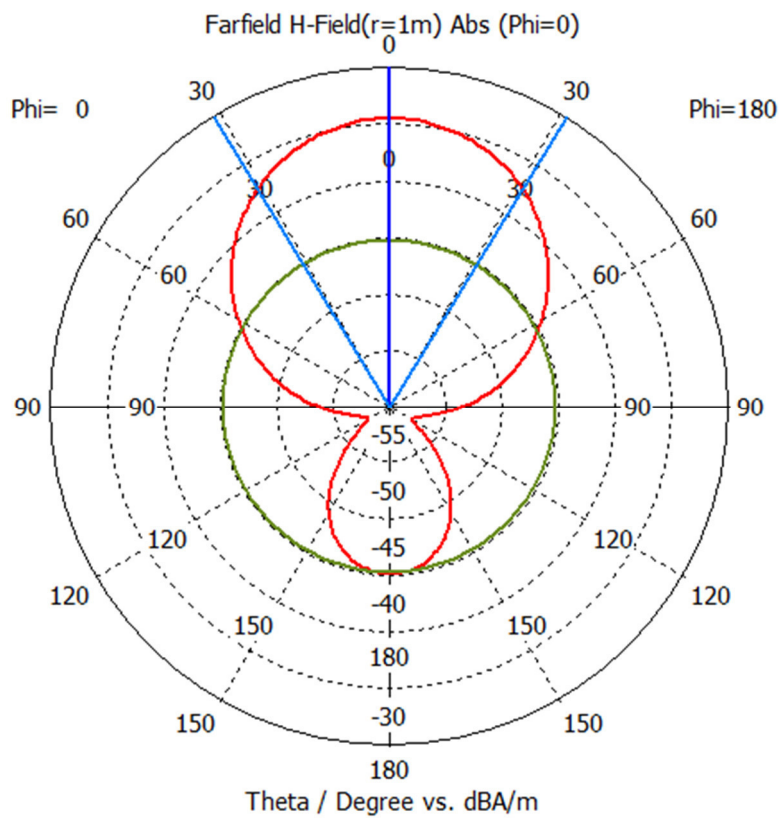
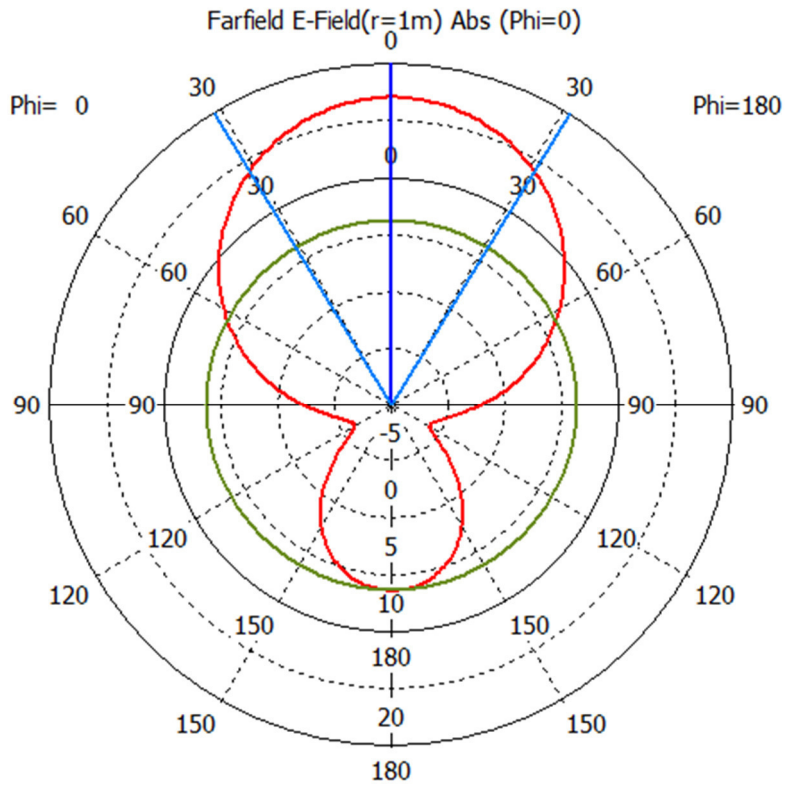


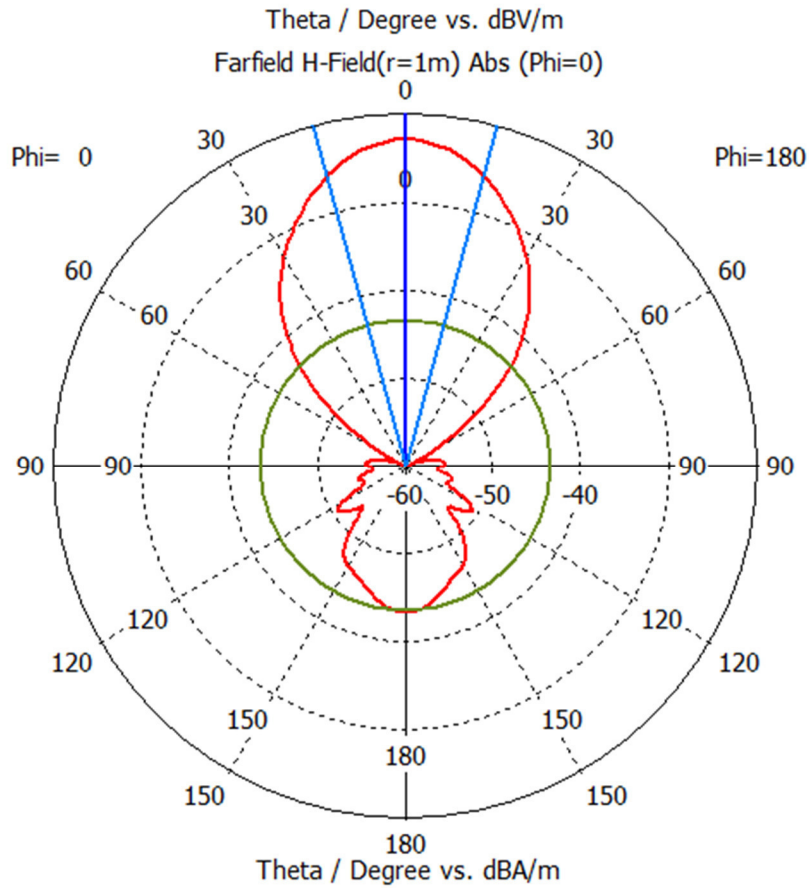
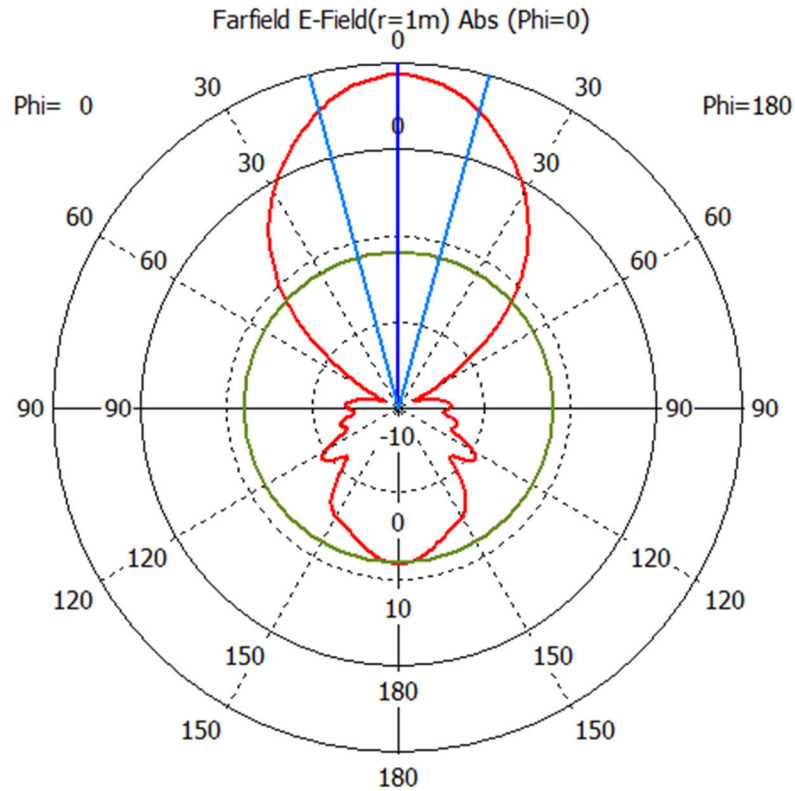
Figure 41: Final result for DRHA

A3. Characteristic of DRHA

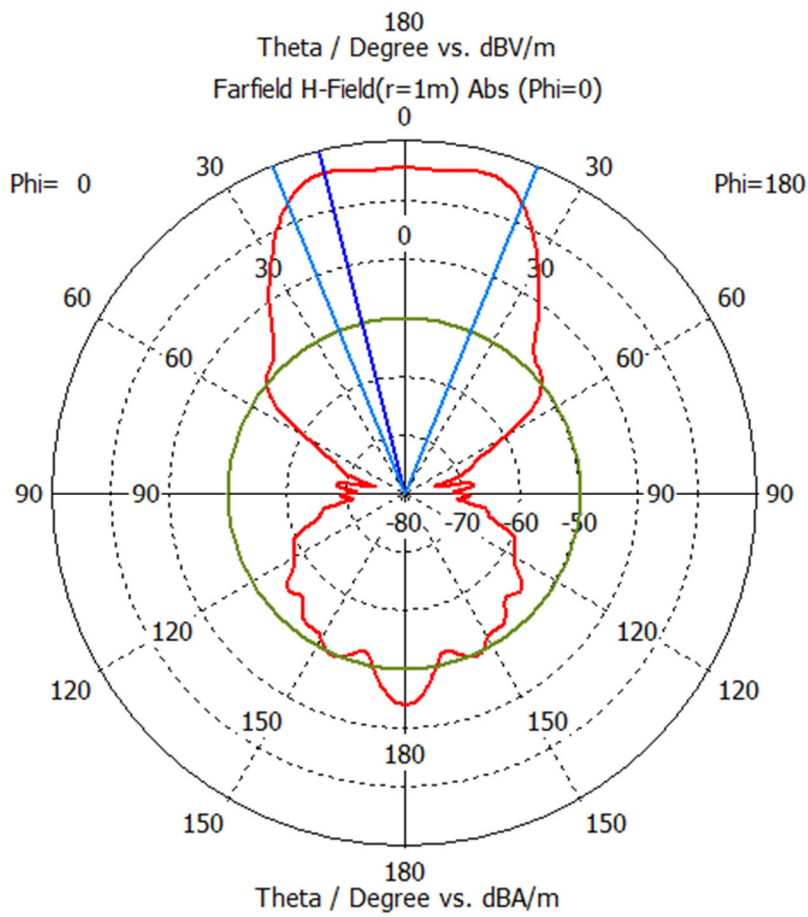
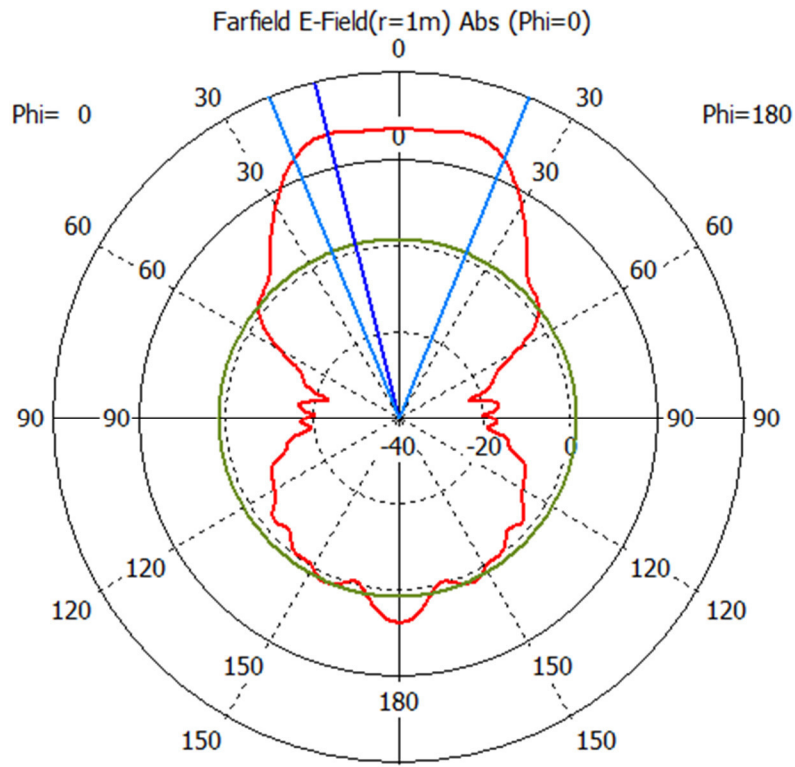
Gain characteristics of the antenna at 1 GHz



Gain characteristics of the antenna at 3,5 GHz

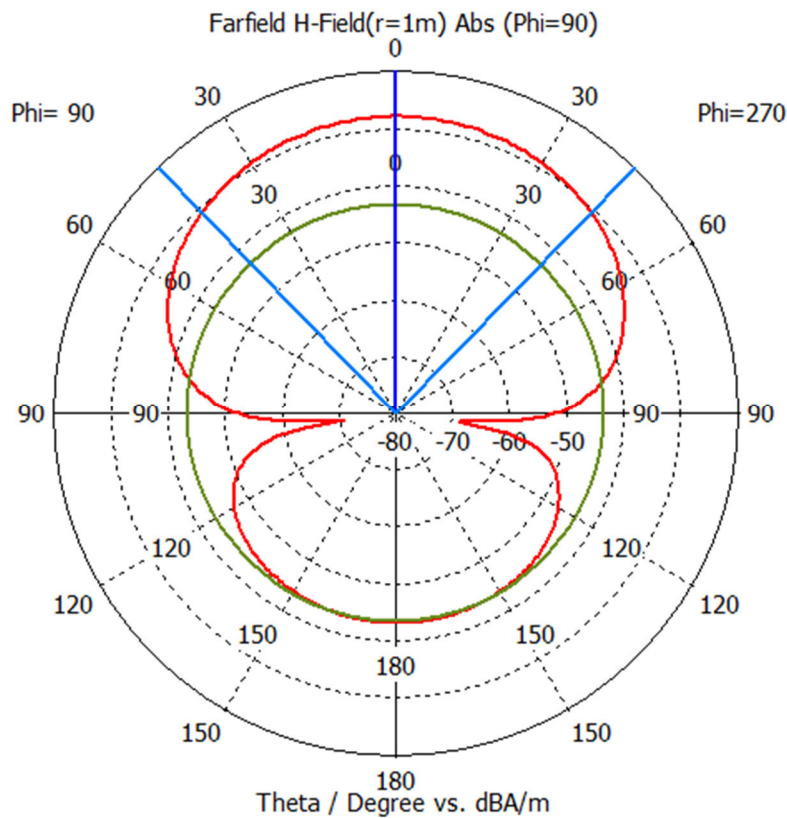
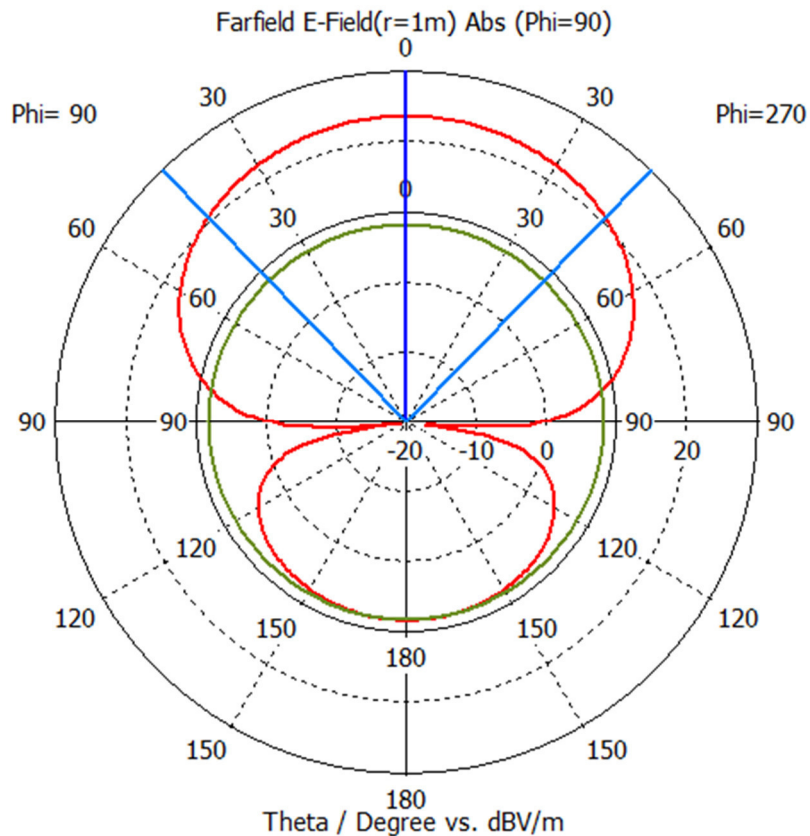


Gain characteristics of the antenna at 6 GHz

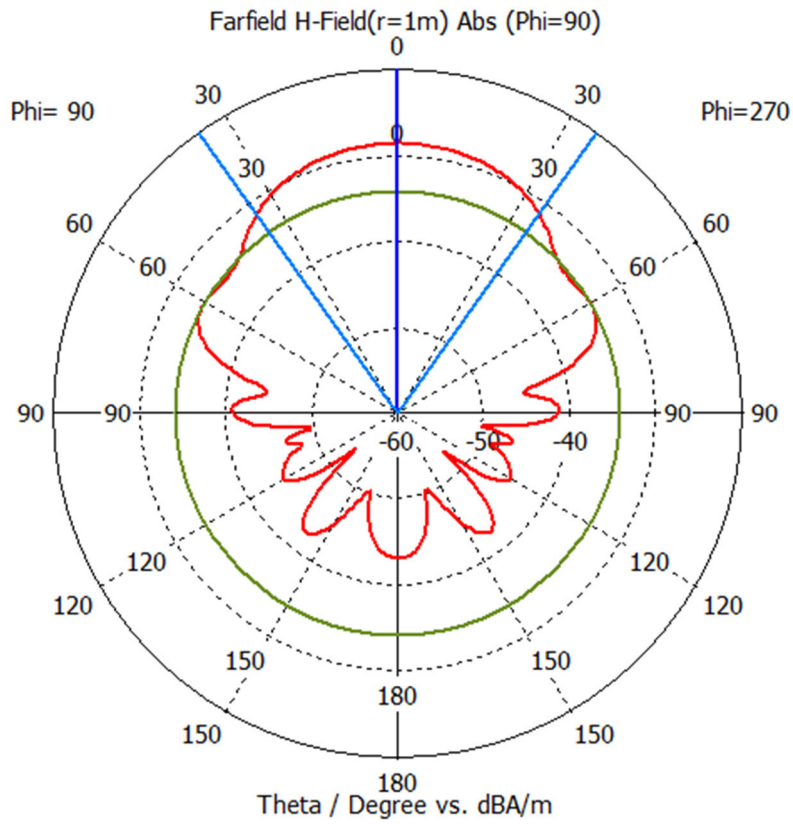
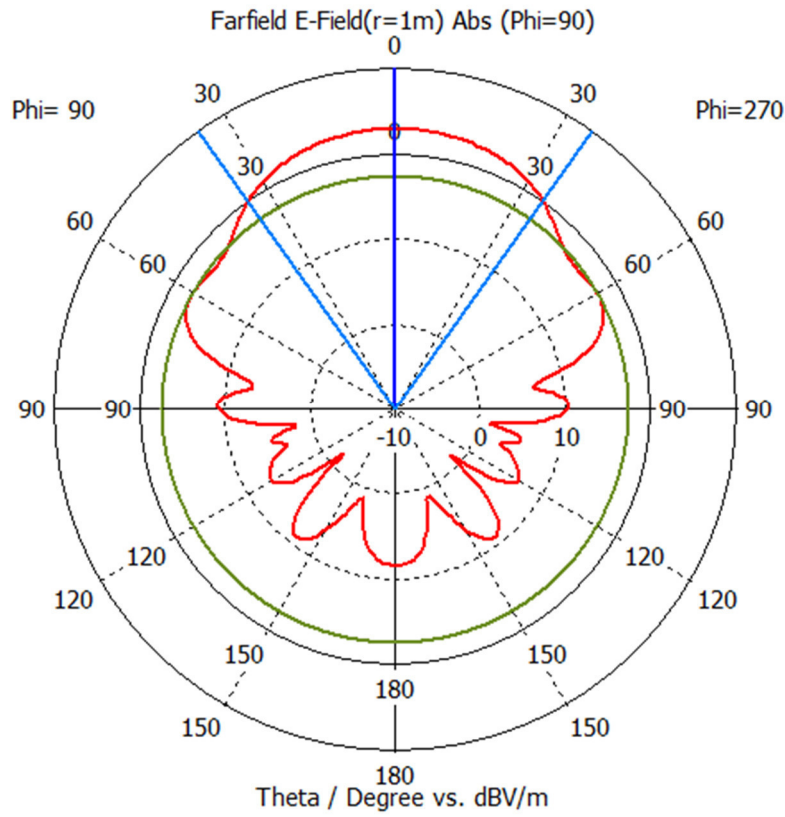


A4. Characteristic of LPDA

Gain characteristics of the antenna at 1 GHz



Gain characteristics of the antenna at 3,5 GHz



Gain characteristics of the antenna at 6 GHz

